Technical Report No. 900-008

INVESTIGATION OF ULTRA HIGH STRENGTH BULK GLASS

Final Report
15 April 1966

by

Robert O. Teeg, Gordon L. Zucker
and Robert W. Hallman

Prepared under Contract NOw 65-0388-f for the Bureau of Naval Weapons, Department of the Navy, by Teeg Research, Inc. (formerly Cadillac Gage Research), 20316 Hoover Road, Detroit, Michigan 48205

Technical Report No. 900-008

INVESTIGATION OF ULTRA HIGH STRENGTH BULK GLASS

Final Report
15 April 1966

by

Robert O. Teeg, Gordon L. Zucker
and Robert W. Hallman

Prepared under Contract NOw 65-0388-f for the Bureau of Naval Weapons, Department of the Navy, by Teeg Research, Inc. (formerly Cadillac Gage Research), 20316 Hoover Road, Detroit, Michigan 48205

TABLE OF CONTENTS

	Page
I. INTRODUCTION	1
II. BOROSILICATE GLASSES	6
A. TENSILE STRENGTH TEST METHODS	6
Sample Selection	6
Cleaning and Etching	6
Coating and Thermal Treatment	7
Testing	7
Strength Determination	9
B. TEMPERATURE DEPENDENCE OF TENSILE STRENGTH OF 7740-8363 COMPOSITE	14
8363 Lead-Silicate Coating	17
8363-7740 Interface	17
Effect of Composition	21
Effect of Loading Rate on the Temperature Dependence of Tensile Strength of 7740 Borosilicate Glass	25
Effect of Chemisorbed Water on Tensile Strength of 7740 Glass	28
C. DISCUSSION	35
III. ELECTRICAL PROPERTIES OF 7740 BOROSILICATE GLASS	37
A. DIELECTRIC CONSTANT AND LOSS TANGENT MEASUREMENTS	40
B. ELECTRICAL CONDUCTIVITY MEASUREMENTS	46
C. DISCUSSION AND FURTHER EXPERIMENTS	55
IV. LOW MELTING POINT GLASSES	60
A. MATERIAL PREPARATION	60
Purification by Distillation	60
Casting	66
B. EVALUATION OF MATERIAL	67
Density Measurement	67
Infrared Transmission	69
C. LOW MELTING POINT GLASS COATINGS	73
LITERATURE CITED	74

SUMMARY

A technique for achieving the high inherent strength of bulk glass is developed. The procedure consists of coating the bulk material with a related glass which remains fluid throughout the temperature range of strength testing. The coating glass is sufficiently similar to the bulk material to provide a continuous viscosity gradient between the bulk material and the fluid coating. A viscosity gradient of this kind prevents both initiation and propagation of surface flaws and should effectively eliminate the influence of atmospheric attack. Since the viscosity gradient on the periphery of the test rod precludes the possibility that surface effects have any significant influence on the observed strength values, this technique is both a research tool for observing the inherent strength of glass and a method of engineering interest with potential structural applications.

Tests performed on 4-6mm diameter rods of borosilicate glass (Corning 7740 and 7720) coated with a lead silicate glass (8363) result in strength values up to 265 kg/mm^2 at temperatures well below their strain points. It is concluded that at these temperatures the observed strength values represent the intrinsic bulk strength of this glass. In both borosilicates the tensile strength is observed to increase as the temperature is lowered from 600°C, reach a maximum value (at about 450°C for 7740 and 420°C for 7720), and then decidedly decrease below the T_{max}.

Studies of the coating material, coating-core interface, and thermal history indicate that these are not factor contributing to the decline in strength at lower temperatures. Removal of chemisorbed water (about 50% of total) and variations in the loading rate (by a factor of 100) are likewise found to have little effect on strength levels. That none of the above factors appears to significantly influence the strength-temperature transformation suggests the possibility that a structural transition in the bulk material may be a cause of the observed strength decrease. This possibility is investigated by measuring the electrical conductivity, loss tangent, and dielectric constant, over the relevant temperature range. The evidence obtained from these studies, although inconclusive, does suggest that the temperature dependence of bulk structure is a probable mechanism.

Concurrent work is performed to explore the feasibility of high strength room temperature bulk glass composites. A distillation method is developed to provide arsenic sulfur glasses of rigorously controlled composition. Compatible coatings which remain fluid down to room temperature and below are also developed by third element additions to As_2S_3. A procedure for manufacturing coated arsenic trisulfide rods in quantities sufficient for extensive strength testing is established.

I. INTRODUCTION

Among common structural materials, glass is one of the most widely used and least understood. Its great utility is the result of a large number of desirable properties such as transparency, corrosion resistance, low temperature coefficient of expansion, and, perhaps most important, great abundance of cheap raw materials. Besides these, glass is a comparatively light weight material having a density comparable to aluminum. In theory, glass should also have a strength comparable or greater than that of most metals. Taken together, these points suggest the possibility of far greater utilization than is now the case. In practice, however, glass is perhaps best known for its brittleness, low measured tensile strength, and capricious fracture and fatigue characteristics. To reconcile this difference between theory and experience, workers in the field were led ultimately to examine the influence of surface damage on the mechanical properties of glass. The reasoning that led to this approach is not known though it is probably likely that the spectacular ease with which window glass can be "cut" was a starting point.

Since introduction of the surface crack concept, a great deal of work has been done in attempts to elucidate the microscopic aspects of crack origin and propagation with the result that strengths observed in various specially prepared samples, such as freshly drawn fibres, have approached theoretical values. This report summarizes work done on a unique method for controlling the surface environment of glass which, because it is not contingent on geometrical properties such as small surface area, shows potential for general applicability in high strength glass configurations of arbitrary size and shape.

The theoretical tensile strength of many silicate glasses and fused silica, based on idealized structural models, is of the order of 10-20% of Young's Modulus or 1-2 million psi (700-1400 kg/mm^2). These values are about three orders of magnitude greater than those associated with ordinary glass. To explain this discrepancy Griffith [1] postulated that the low tensile strengths which are actually

observed in bulk glasses result from stress concentrations in microcracks. Considering a microcrack as an elliptic hole in a stressed plate Griffith obtained the following relation for the stress required for crack propagation

$$\sigma = 2 \left(\frac{S E}{\pi \ell} \right)^{\frac{1}{2}} \qquad (1)$$

where ℓ is the length of the crack, S the surface tension, and E the modulus of elasticity. Although direct verification of the Griffith formula has been difficult, several indirect methods indicate that its form is basically sound.

Note that the Griffith relation predicts that the tensile strength should vary as the inverse square root of ℓ, the long dimension of the crack. We can therefore expect geometries of small surface area, where the chance of a flaw being present is small, to exhibit strength values greater than the bulk material. This was shown to be the case by Griffith who, by working with thin glass fibers, obtained strength values of 630 kg/mm^2, or about one half of the maximum theoretical strength value. For a time, however, these results remained controversial since an apparent "size effect" was also observed suggesting that the method of sample preparation introduced a tendency for flaws to orient parallel to the direction of tension. This was disproved by Otto and Preston [2] who tested fibres in torsion and tension and found equal strengths both parallel to and at 45° to the fibre axis. A proposal due to Tool [3] wherein he suggests that the strength of small-diameter fibres results from an oriented chain molecular structure enhanced by the drawing process appears, likewise, to be contrary to the result obtained by Otto and Preston. The work performed during this study further demonstrates that high strength need not be associated with processing variables encountered in fibre manufacture but is rather an inherent property of bulk glass.

Still more support for the Griffith theory is provided by microhardness experiments. In these a ball is pressed against a plane glass surface

until fracture occurs. If the glass surface had uniform strength, the pressure required for fracture would increase as the square of the diameter of the ball. Instead it is found that glass endures higher stress under a small ball than a large one. In that a flaw is more likely to be found in the contact area under a large ball, the greater stresses observed with smaller balls suggest, again, that flaws or surface cracks are the significant strength controlling factors in ordinary glass. Recent review of the subject include those of Hillig, [4] Ernsberger, [5] Zijlstra, [6] and Bartenev. [7]

While the effect of microcracks on the ultimate strength of glass appears to be adequately, if somewhat roughly, described by the Griffith theory, their origin is less well understood and is probably the result of a number of competing processes including

(i) mechanical contact with other materials,

(ii) atmospheric or other chemical attack, and

(iii) thermal effects.

Once a crack is initiated from a surface microdefect, a very low stress is required for its propagation through the matrix.

If, however, the surface is modified in such a way that microcracks cannot be initiated the mechanical properties of glass should be significantly enhanced and more representative of bulk rather than surface properties. This can be accomplished, as shown schematically in Figure 1, by the fabrication of a composite structure in which a viscosity gradient is produced in the outer periphery of the test rod, the outermost surface having a softening point below the test temperature. The outer periphery will thus be relatively fluid permitting neither initiation nor propagation of a microcrack to the relatively strong inner core material. Experiments performed during this study indicate that rods treated in this manner do, in fact, exhibit strength approaching theoretical values.

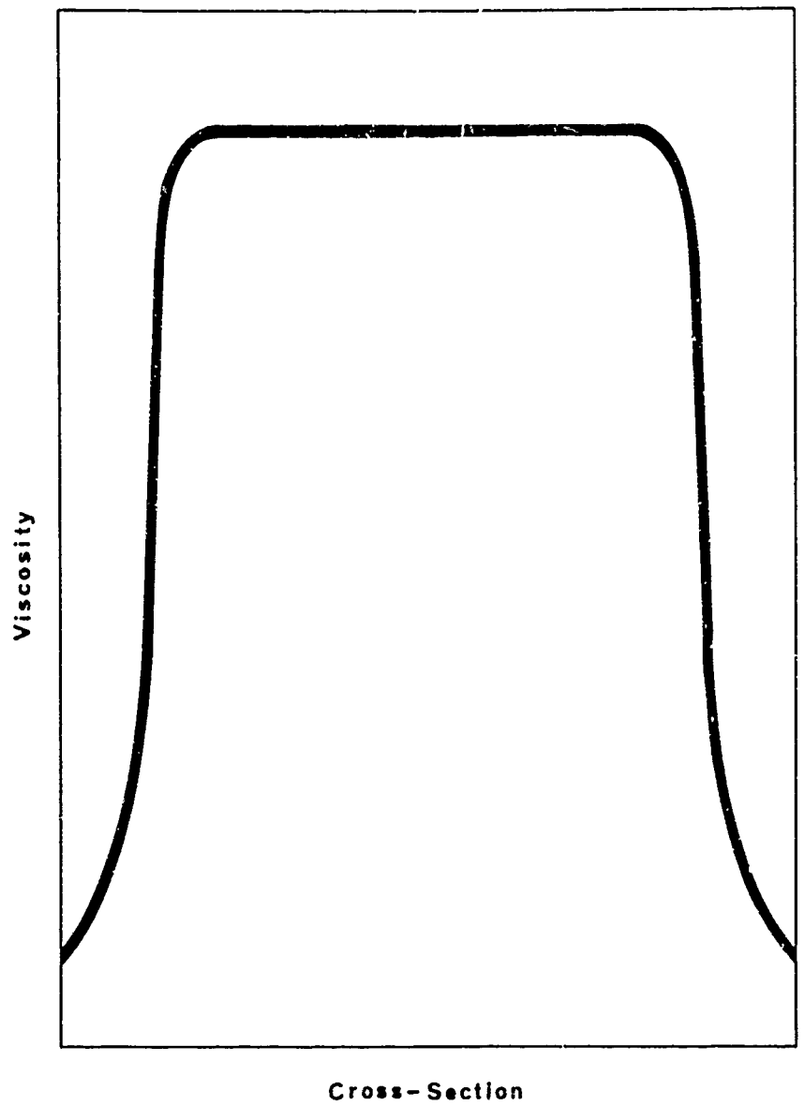

Figure 1. Schematic of viscosity gradient in composite.

Besides its potential application to the development of high strength structural components this technique has the advantage that strengths observed are more representative of the properties of the bulk material than would be the case with untreated samples whose measured strengths, as indicated above, are governed by surface conditions. Also, some of the ambiguities inherent in work with fibres are eliminated in this procedure in that only a small portion of the test sample is altered in the experiment while the strength bearing core remains unaffected. In essence, then, this method provides a means for correlating meaningful strength values with material parameters such as chemical composition, impurity content, and electrical properties, each of which can be readily altered in the course of a materials study aimed at delineating possible mechanisms which govern the intrinsic strength of glass.

Since this method of eliminating the deleterious surface effects in glass is both a research technique and a means for improving the strength of glass, with possible structural applications, the work performed during the past year exhibits a duality of emphasis consisting of

(i) development and improvement of measuring techniques and isolation of operative strength variables and

(ii) development of methods for production of low temperature glasses of known chemical composition.

The work performed on the borosilicates consists of the establishment of test procedures and an investigation of operative strength variables using commercially available materials. The effects on tensile strength of the coating, coating-core interface, composition, loading rate, chemisorbed water, and thermal cycling are determined as functions of temperature. Extensive electrical measurements were performed on Corning 7740 as part of an effort to correlate other physical properties with the temperature-strength transformation observed at about 450°C.

Low melting point glass studies were initiated by developing methods for production of pure arsenic trisulfide glass together with techniques for monitoring sample quality.

II. BOROSILICATE GLASSES

Earlier work in this laboratory on 7740 borosilicate glass rods coated with 8363 lead silicate glass revealed an interesting strength-temperature relation. Between 600°and 450°C the strength of coated samples is found to increase with decreasing temperature, reaching a maximum value at about 450°C; at lower temperatures the strength decreases rapidly suggesting a transformation in the composite structure. To further investigate this phenomenon a systematic study of the strength-temperature characteristics of 7740 is performed.

A. TENSILE STRENGTH TEST METHOD

In most studies of glass utilizing commercially available samples there are usually more variables than even the most elaborately controlled experiment can possibly isolate. The composition is usually nominal and the thermal history unknown. To minimize the influence of thermal history and reduce the possibility of introducing new unknowns, rigorous selection and test procedures are necessary. The preparation and testing procedure used in this study is highly effective in reducing experimental scatter.

Sample Selection

A selected rod, from which test samples are cut, is one which has been visually examined along its length and found to be free from severe flaws such as bubbles, deep scratches, and channel voids. An end section of this rod, approximately six inches in length, is scribed with a batch and rod number, then cut and stored as a control sample. The samples for testing are then obtained by what are now essentially center cuts from the remaining length of rod. These test samples are each given an individual screening which excludes samples with bubbles and channel voids which would not be eliminated by the subsequent preparation treatment.

Cleaning and Etching

Test samples are considered as individual units and at no time are

the samples permitted to contact each other. Handling is minimized and,when necessary,only the ends of the sample are gripped. Cleaned rods are placed in a polyethylene jig designed for etching in an HF bath. The selection of an etchant is based on work performed by B. Proctor [8]. After experimenting with various combinations of HF, HCl, and H_2SO_4, Proctor found that a solution containing 15% HF, 15% H_2SO_4 is most effective. The strength of 8mm rods increases with increasing surface removal up to a depth of 0.4mm after which additional removal does not appreciably effect the strength.

Initial experiments on 7740 were performed using a 15% HF, 15% H_2SO_4 etchant. Diameter removal is monitored by periodic micrometer measurements. A dissolution rate of 0.2mm/hr was found to be too slow and a 40% HF solution was substituted. This etchant was faster and did not appear to have any detrimental effects on 7740. Unfortunately, the 40% HF left sizable deposits of a white precipitate when used for 7720 rods. The etchant was therefore modified to contain 53% HF and 37% HCl. This is found to eliminate precipitate deposits.

Coating and Thermal Treatment

Prepared rods are immersed in a thermally and compositionally homogenized bath of the coating glass. The elapsed time between completion of preparation and immersion is noted. The immersed samples are not permitted to come into contact during the coating process and are agitated periodically to insure uniform dissolution. The time in the melt (4 hours) and melt temperature (600°C) is determined by the desired material removal, based on working curves for dissolution rate.

Testing

Treated samples are tested in bending by a 3 point loading technique. A photograph of the fixture designed for this purpose is shown in Figure 2. Testing is performed by a modified Instron Universal Tensile Tester with a specially designed thermal chamber to

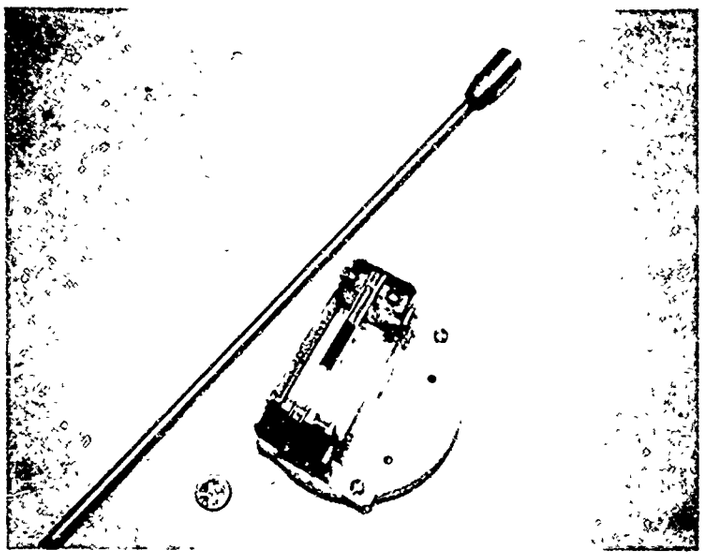

Figure 2. Bending Test Fixture

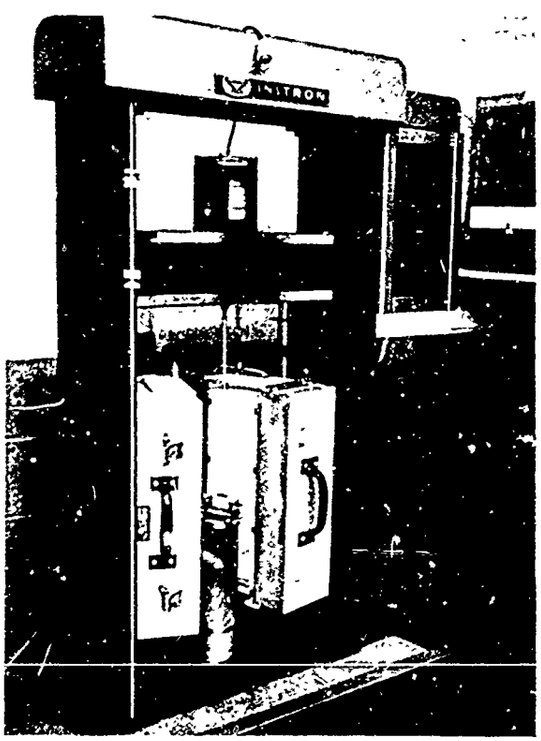

Figure 3. Complete Testing Facility

provide temperature control $\pm$ 2°C up to 1,000°C. Figure 3 shows the complete testing setup. Fractured or bent test samples are recovered, when possible, and mounted in epoxy. Polished specimen cross-sections are examined and measured by metallographic techniques.

Strength Determination

For a circular beam in three point loading, Figure 4(a), the maximum tensile stress is given by

$$\sigma_m = \frac{MD}{2I} \qquad (2)$$

where M is the maximum bending moment, D the diameter, and $I = \pi D^4/64$ the moment of inertia of the cross sectional area relative to the neutral axis. For small deflections the lateral loads arising at the fixed supports can be neglected and we obtain for the bending moment

$$M = \frac{P X (L-X)}{L} \qquad (3)$$

which, for central loading, reduces to

$$M = \frac{PL}{4} \qquad (4)$$

$$\sigma_m = \frac{PLD}{8I} = \frac{8}{\pi} \frac{PL}{D^3} \qquad (5)$$

This formula is used to compute the maximum tensile stress.

In this approximation (i. e., small deflection) two sources of experimental error are possible:

(i) off-center loading and

(ii) uncertainty in the determination of the rod diameter

Their relative magnitudes can be estimated by computing the total differential.

$$\Delta \sigma_m = \frac{\partial \sigma_m}{\partial D} (\Delta D) + \frac{\partial \sigma_m}{\partial x} (\Delta x) \qquad (6)$$

The maximum relative error is, after differentiation,

$$\frac{\Delta \sigma_m}{\sigma_m} = 3 \left(\frac{\Delta D}{D} \right) + 8 \left| \frac{\Delta x}{L} \right|^2 \qquad (7)$$

from which it is apparent that uncertainties in the diameter introduce the more serious error. Except in the case of gross misalignment, which would be readily apparent, the second order term, arising from off-center loading, can be neglected. Since the last significant figure obtained by metallographic measurement is 0.1mm, the maximum error for a 4 mm diameter rod is about 8%. The actual error introduced is probably somewhat less than this since one additional, though somewhat uncertain, figure can be obtained by interpolation.

The error introduced by use of the simple small deflection approximation is more difficult to estimate. It is clear, however, that use of the simple formula will give lower ultimate strength values than a more sophisticated treatment. This can be seen best from Figure 4(b); the lateral forces arising from the fixed supports can only increase the bending moment at the center of the rod to some value greater than the PL/4 obtained in the simple case. An estimate of the magnitude of this effect can be obtained by assuming that near the breaking stress the loading on the test rods is as shown in Figure 4(c). If we further assume that the angular deflection at the support is given by the simple formula

$$\theta - \frac{P L^2}{16 E I} \qquad (8)$$

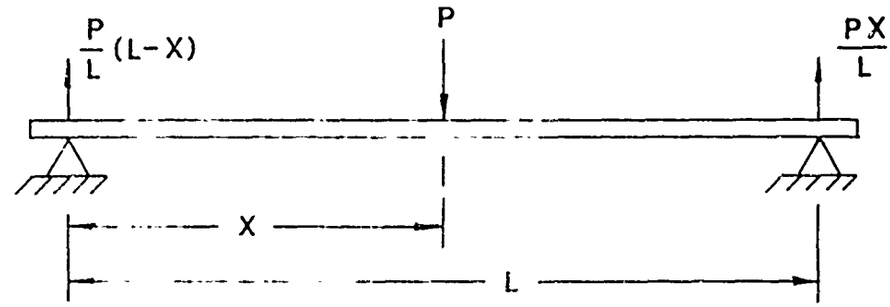

(a)

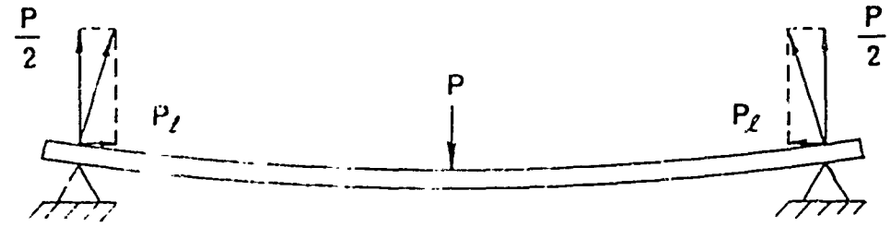

(b)

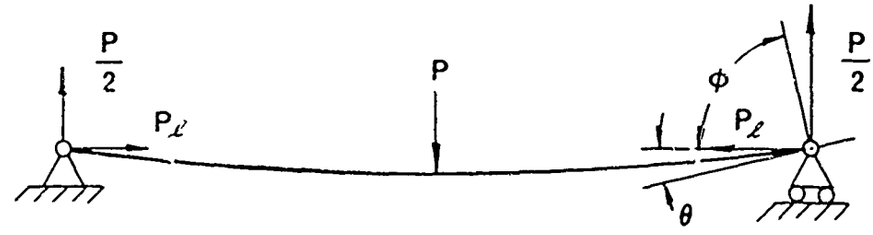

(c)

Figure 4. Three Point Loading Diagrams. (a) Simple Loading, Small Deflection. (b) Non-ideal Loading, Lateral Loads at Supports. (c) Model Used in Estimating Effects of Large Deflection.

the lateral load is

$$P_\ell = \frac{P}{2} \cot\phi \cong \frac{P}{2} \cos\phi = \frac{P}{2} \cos\left(\frac{\pi}{2} - \theta\right) = \frac{P}{2} \sin\theta$$

$$\cong \frac{P}{2} \theta$$

For central loading of this configuration, the maximum bending moment is given by Timoshenko [9] as

$$M_{max} = \frac{P L}{4} \quad \frac{\tan u}{u} \tag{9}$$

where

$$u^2 = \frac{P_\ell}{4} \cdot \frac{L^2}{E I} \tag{10}$$

which, after substitution for θ and I, gives

$$u = \frac{32}{\pi} \cdot \frac{P L^2}{E D^4} \tag{11}$$

Using the values

$$P = 50 \text{ kg}$$

$$L = 76 \text{ mm}$$

$$E = 6.3 \times 10^3 \text{ kg/mm}^2$$

$$D = 4 \text{ mm}$$

which are representative of our test conditions, we obtain

$$u = \frac{32}{\pi} \cdot \frac{(50)\ (76)^2}{6.3 \times 10^3\ (4)^4} = 0.32 \quad \text{(radians)}$$

and

$$M_{max} = \frac{P\,L}{4} \cdot \frac{\tan u}{u} = \frac{P\,L}{4} \cdot \quad (1.033)$$

which is about 3% greater than the maximum moment obtained in the simple case.

A further indication of the adequacy of the simple formulae for the test conditions in this work can be obtained by comparing observed and calculated values of maximum deflection. A 4.1mm diameter rod is observed to fracture under a 48 kg load after undergoing a maximum deflection of 5.5mm. The simple formula for maximum deflection for three point central loading is

$$y_{max} = \frac{P\,L^3}{48\,E\,I} = \frac{4}{3\pi} \frac{P\,L^3}{E\,D^4} \qquad (12)$$

which gives, with $E = 6.3 \times 10^3$ kg/mm^2,

$$y_{max} = \frac{4}{3\pi} \frac{(48)\ (76)^3}{(6.3 \times 10^3)\ (4.1)^4} \cong 5.0 \text{ mm}$$

This value is in good agreement with the observed value of 5.5mm if allowance is made for uncertainties in the diameter and Young's modulus.

It should be noted that the use of "tensile stress" in this report refers to the maximum stress exerted on the outermost fibers of a rod tested in bending. The values reported here may be correctly compared to modulus of rupture values reported elsewhere, since both terms refer to the ratio of the bending moment to section modulus. The nomenclature used in this study is considered more appropriate since, as will be shown, several samples exhibit yielding behavior for which the use of "rupture" would be misleading.

B. TEMPERATURE DEPENDENCE OF TENSILE STRENGTH OF 7740-8363 COMPOSITE

The temperature dependence of tensile strength of 7740 borosilicate glass, coated and treated as described in the previous section, is shown in Figure 5. The strength increases with decreasing temperature between 600°C and 450°C; below 450°C the strength decreases rapidly with further reduction in temperature. Analysis of the load deflection curves results in the two classifications of fracture data indicated in Figure 5:

(i) Fracture with no detectable deviation from load-deflection linearity. An example of this behavior is shown in Figure 6(a). In 7740 borosilicate glass this is usually observed below 450°C.

(ii) Fracture after deviation from load-deflection linearity. Figure 6(b). This behavior is usually observed above 450°C.

Between 350°C and 450°C, over 70% of the samples tested fracture without deviation from load-deflection linearity while over 70% of samples tested above 450°C fracture after deviation from load-deflection linearity. The temperature region near 450°C is thus peculiar in that there is a change in both the trend of the strength-temperature data and the mode of fracture. This temperature region will be referred to hereafter as the strength-temperature transformation.

The magnitude of the measured strengths validates the original assumption that the method used in this study gives the intrinsic strength of glass and not values dependent on surface conditions. Since the confines of surface flaws are not therefore expected to dominate the temperature dependence of strength, the strength-temperature transformation is probably the result of a change in the composite. The origin of the strength transformation is examined by considering the influence of the following factors:

(i) the 8363 lead silicate coating,

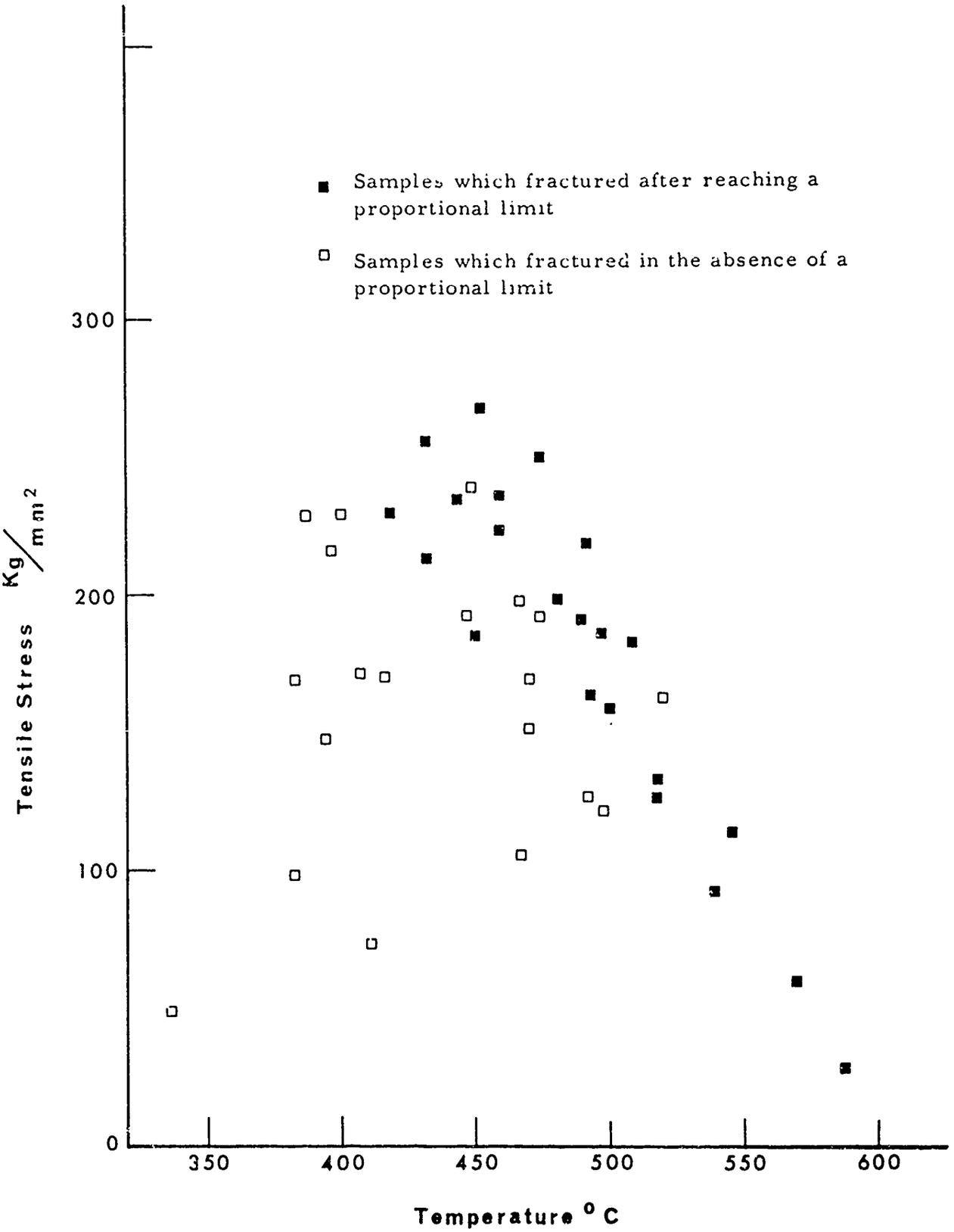

Figure 5. Temperature dependence of tensile strength of 7740 borosilicate glass.

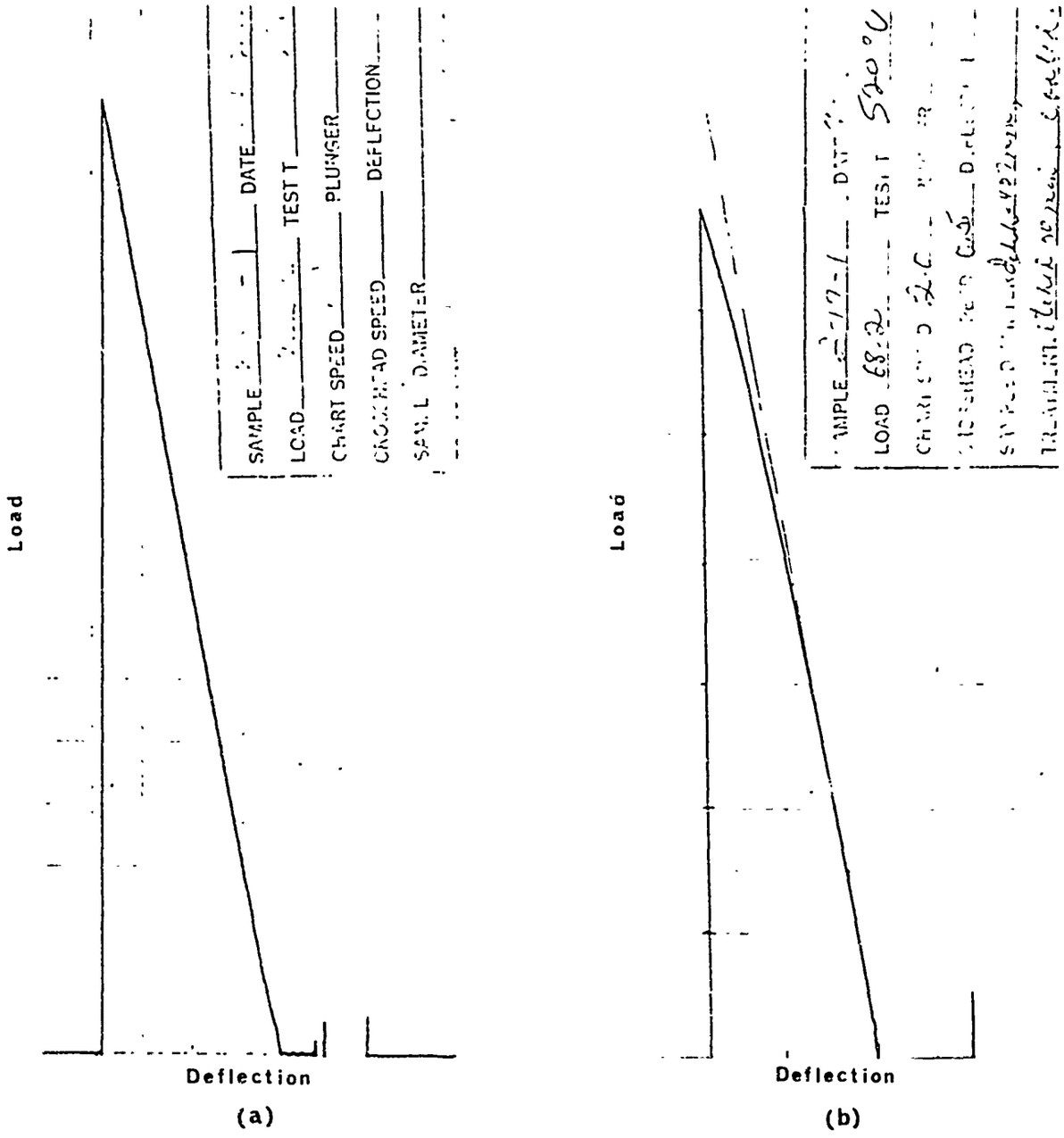

Figure 6. Load-deflection charts for two 7740 samples
(a) 390°C. (b) 520°C

(ii) the 8363-7740 interface, and

(iii) the 7740 borosilicate matrix.

8363 Lead-Silicate Coating

The 8363 lead silicate glass is chosen as the coating material because of its viscosity-temperature characteristics, Figure 7(a), and its ability to form a continuous interface with the 7740 borosilicate core. As shown in Figure 7(b), the coating remains fluid in the temperature interval over which samples are tested. That is, the low temperature cut-off chosen (350°C) is such that it eliminates 8363 viscosities which could house flaws of the Griffith type. There is a possibility that prolonged exposure to elevated temperatures might produce deterioriation of the coating glass. This is not evident in various runs during which 8363 glass is held in the 420° to 470°C temperature interval for periods up to 30 hours. Since the coating itself is not a load bearing constituent, its role in the strength temperature transformation is considered negligible.

8363-7740 Interface

The only probable mechanism by which the interfacial region might affect the strength of the 7740-8363 composite is crystallization. For crystallization to occur, the rates of nucleation and growth of crystallites, shown schematically in Figure 8, must be appreciable at or above the test temperature. If this is the case and crystallization does occur in the interface, it is reasonable to expect that the strength level is related to the number and size of crystallites formed in the 7740-8363 alloy interface. That is, under these conditions, the strength levels attained by the composite should be related to the rate of cooling through the temperature range of maximum crystallization power * with slow rates producing more

---

* Crystallization power can be considered, roughly, a combined measure of (i) the rate of formation of crystal nuclei and (ii) the growth rate of crystallites.

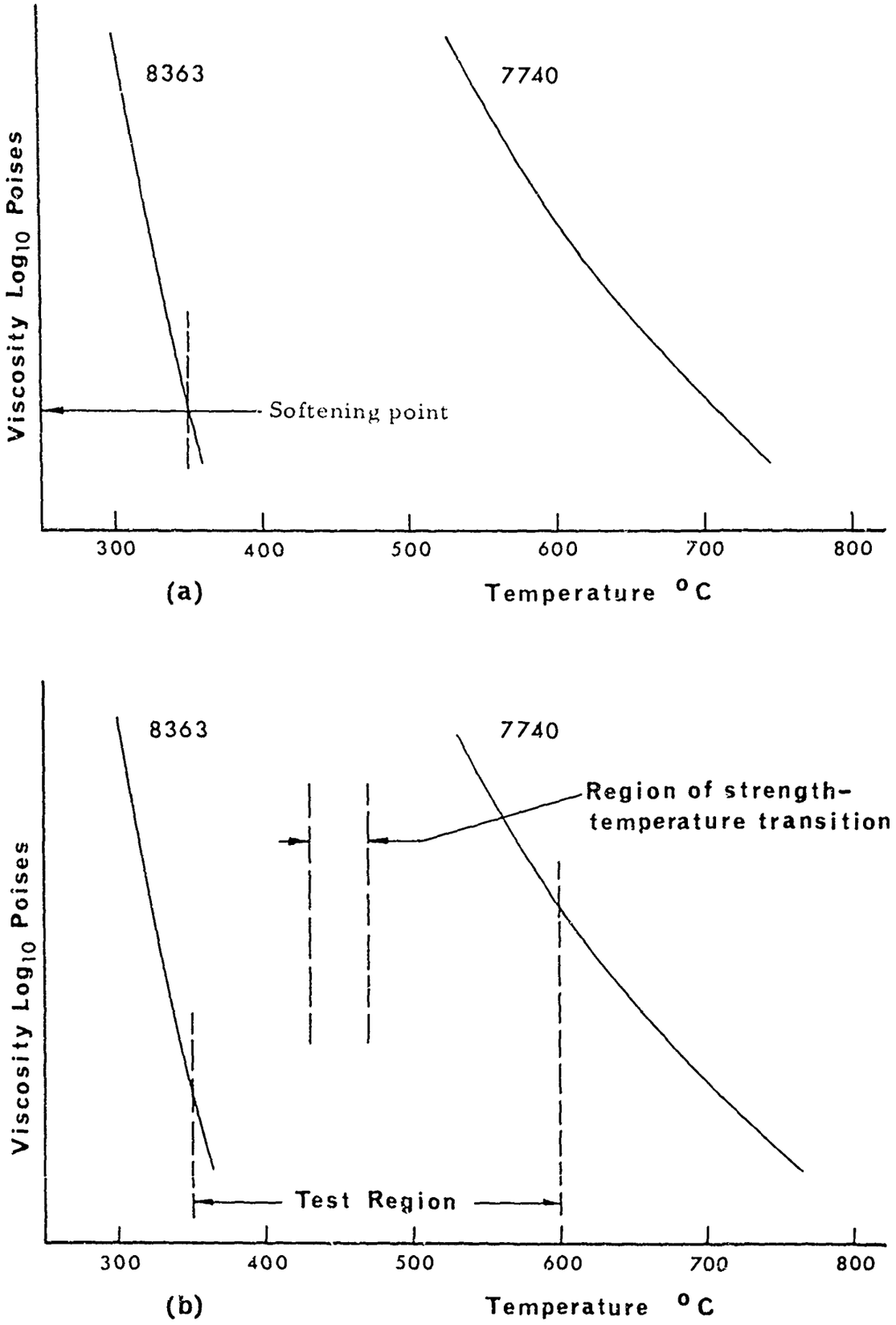

Figure 7. Temperature dependence of viscosity for composite materials.

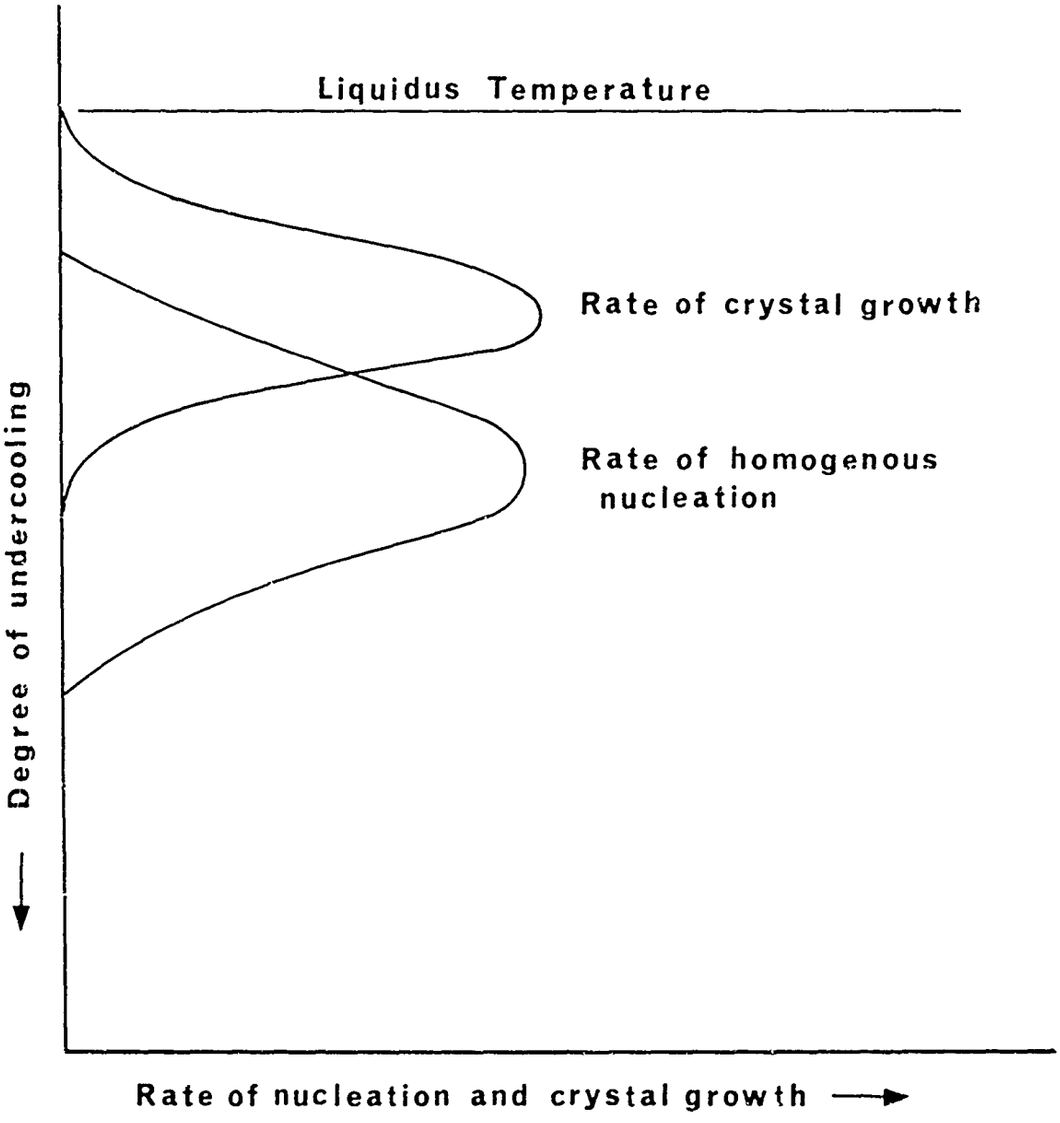

Figure 8. Rates of homogenous nucleation and crystal growth.

crystallization than fast rates. Two severely different cooling rates were used to test this hypothesis. The results are shown in Table I.

TABLE I

	Slow Cool (1°C/min)	Fast Cool (50°C/min)
Treatment Temperature and Time to	600°C (4hours)	600°C (4hours)
Transfer Temperature from 600°C to	600°C	350°C
Test Temperatures °C	418	418
Tensile Strength(Kg/mm^2)	100	125

The strength levels achieved for the samples exposed to the two different cooling rates are not considered to be significantly different from each other or samples tested after direct transfer to the test temperature. In addition, metallographic examination of the 7740-8363 boundary does not reveal any crystal formation or other evidence of interfacial deterioration.

The 8363 coating and the 8363-7740 interfacial region, as examined, are not obviously connected with the strength-temperature transformation observed. To further establish the possible effects of the coating and interface and simultaneously examine the dependence of matrix composition, a similar borosilicate 7720 was tested.

Effect of Composition

TABLE II

Chemical Composition Weight % of
7740 and 7720 Borosilicate Glasses

Constituent Oxides	Corning Nominal	Analysis This Study	Corning Nominal	Analysis This Study
SiO_2	80.5	80.76	73.0	72.58
B_2O_3	12.9	12.16	16.5	15.87
Na_2O	3.8	4.08	4.5	3.65
K_2O	0.4	0.01		0.13
Al_2O_3	2.2	2.51		1.16
PbO			6.0	5.87

The compositional differences between 7740 and 7720 are shown in Table II and a comparison of the viscosity temperature characteristics is given in Figure 9. The temperature dependence of the strength of 7720 borosilicate glass, treated in an identical manner as the 7740, is shown in Figure 10. Note that among samples fracturing after reaching a proportional limit there is a clear exponential increase of tensile strength with decreasing temperature, reaching a maximum at about 410°C. Below 410°C all samples tested show significantly lower strength values, and, perhaps most important, all fracture before reaching the proportional limit. Data for both 7740 and 7720, comparing only samples which exhibit a proportional limit, is shown in Figure 11, from which the generally lower strength of the 7720 and the lower temperature of the strength-temperature transformation is evident.

The differences in the temperatures of maximum strength, prior to the rapid strength decrease, is of particular interest since the coating and very likely the interface are identical in both experiments. The temperatures are respectively 450°C and 410°C in 7740 and 7720 suggesting that the strength reduction is more characteristic

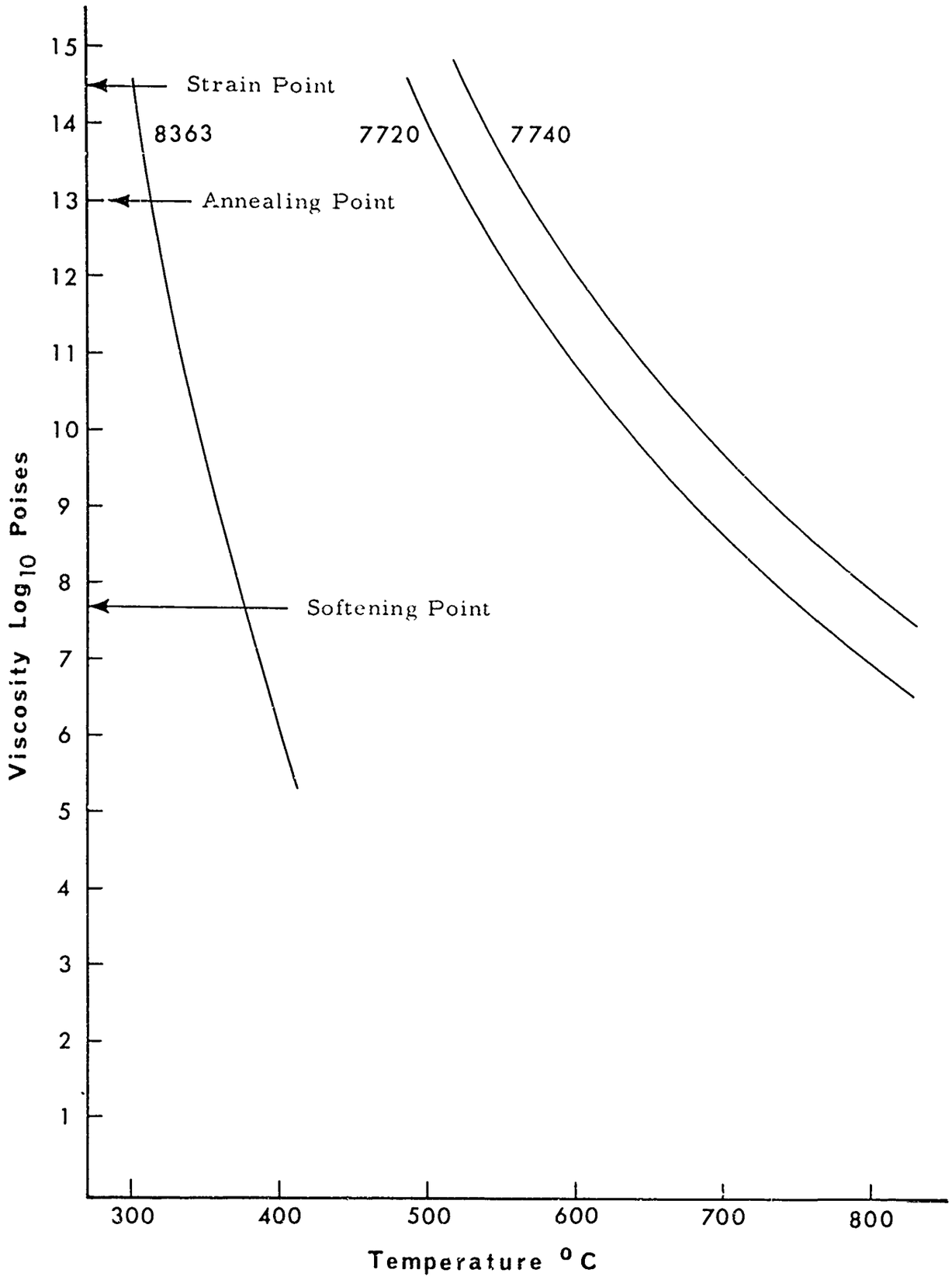

Figure 9. Nominal viscosity-temperature characteristics of 7740, 7720 and 8363.

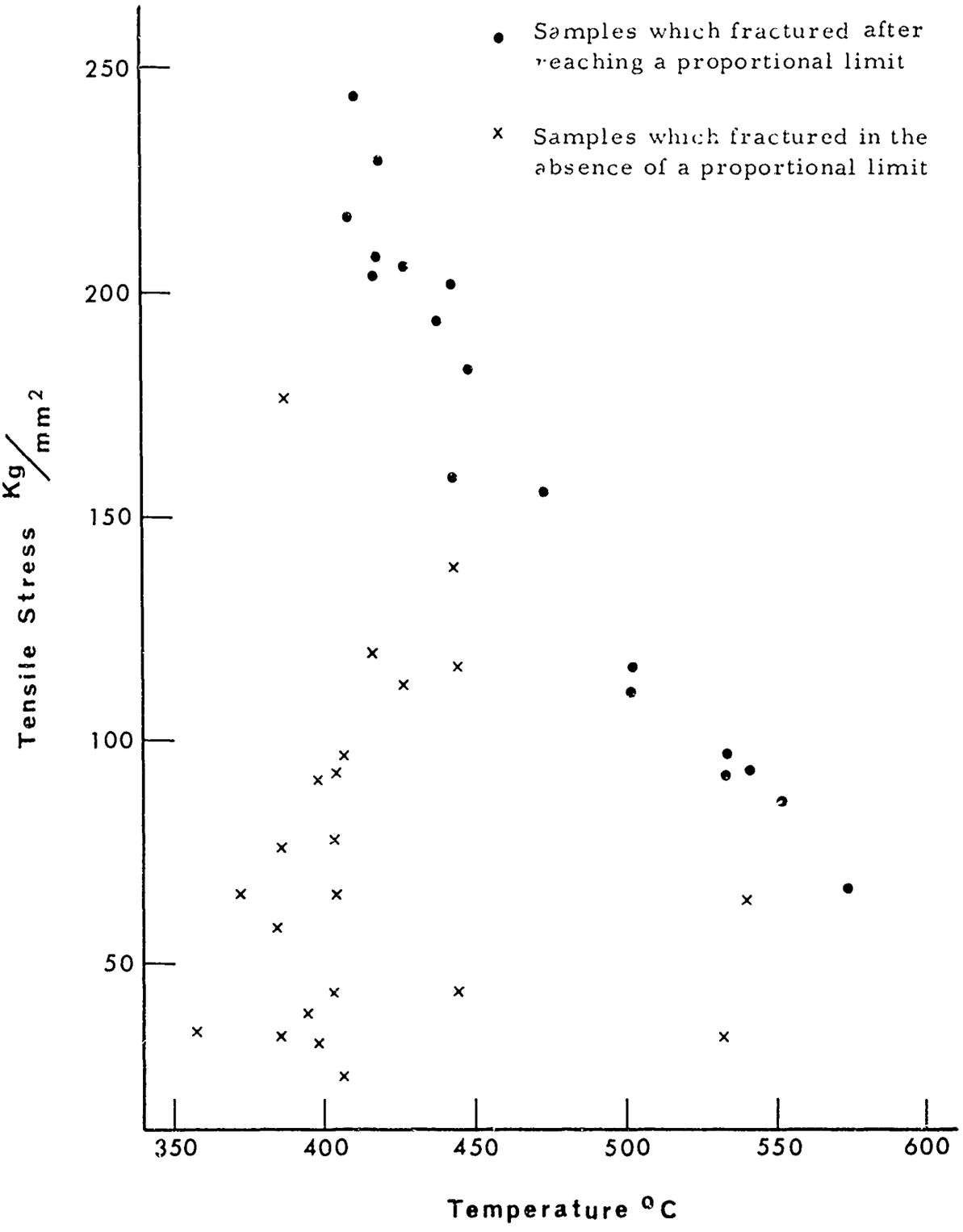

Figure 10. Temperature dependence of tensile strength for 7720 borosilicate glass.

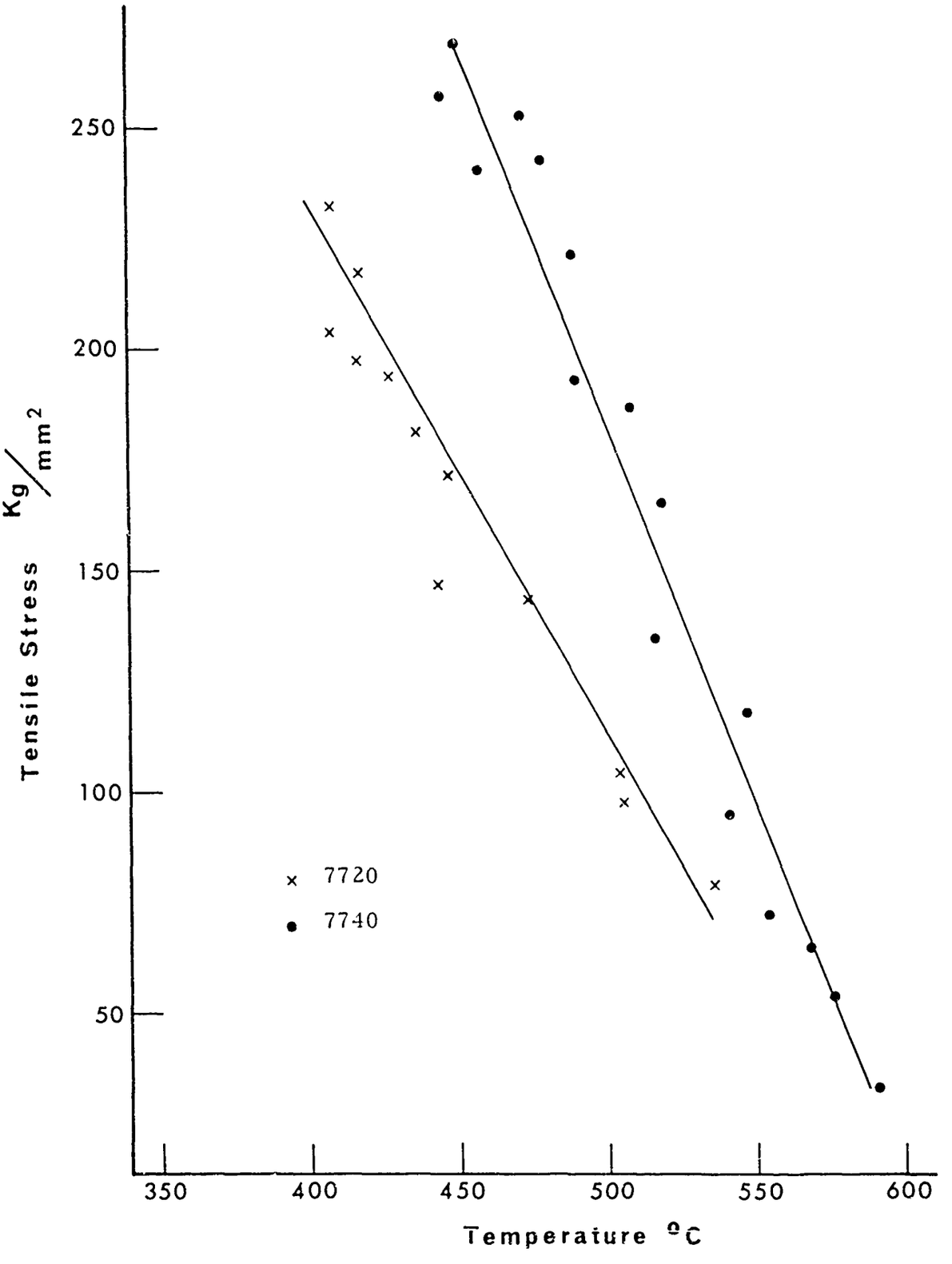

Figure 11. Comparison of temperature dependence of 7720 and 7740 borosilicate glass including only samples which exhibited a proportional limit.

of the solid core than of a change in the coating or a modification of the interface. Of further interest is the fact that the 40°C temperature difference of the two maxima is consistent with differences in the viscosity temperature characteristics--the 7720 achieves a viscosity comparable to that of the 7740 glass at 40°C lower temperature. While the fact that the strength transformation observed in both 7740 and 7720 occurs at temperatures corresponding to the same viscosity may be fortuitous, it does tend to suggest a strength transformation model involving modification of the matrix.

Effect of Loading Rate on the Temperature Dependence of Tensile Strength of 7740 Borosilicate Glass

Several previous investigators [10] have noticed that the strength of glass depends upon the rate at which the load is applied. "Fast" loading rates are found to result in higher measured tensile strength than "slow" loading rates. This result is generally accepted [ ] as due to the time-dependent action of adsorbed water on surface flaws. In the slow loading rate case the deleterious effect of water has more time to act.

Since the coating technique and high test temperature used in this study exlude, or at least inhibit, the possibility of attack by atmospheric constituents such as water vapor, the effect of loading rate was measured as a test of the limits of the existing hypothesis and to gain additional information concerning strength governing mechanisms. The following experiments were performed. Test samples of one lot of the nominal 7740 composition were prepared, tested and analyzed in accordance with the technique described in Section A. Strength-temperature data for this lot were generated at three loading rates:

a. Fast--5.0cm/min

b. Intermediate--0.5cm/min

c. Slow--0.05cm/min

The results of this experiment are shown in Figure 12. The general trends of the strength-temperature curves at the three loading rates indicate that the strength levels achieved are greatest for tne 5.0cm/min rate and least for 0.05cm/min rate. While this result is the same as reported in other investigations the proposed mechanism involving adsorbed water does not seem very likely under these test conditions. It appears more likely that the increase in tensile strength with loading rate may be consistent with the view [11] that glass can, in some sense, be regarded as a very viscous Newtonian fluid--i.e., a fluid in which the viscous stresses (tending to oppose distortion) are proportional to the rate of distortion.

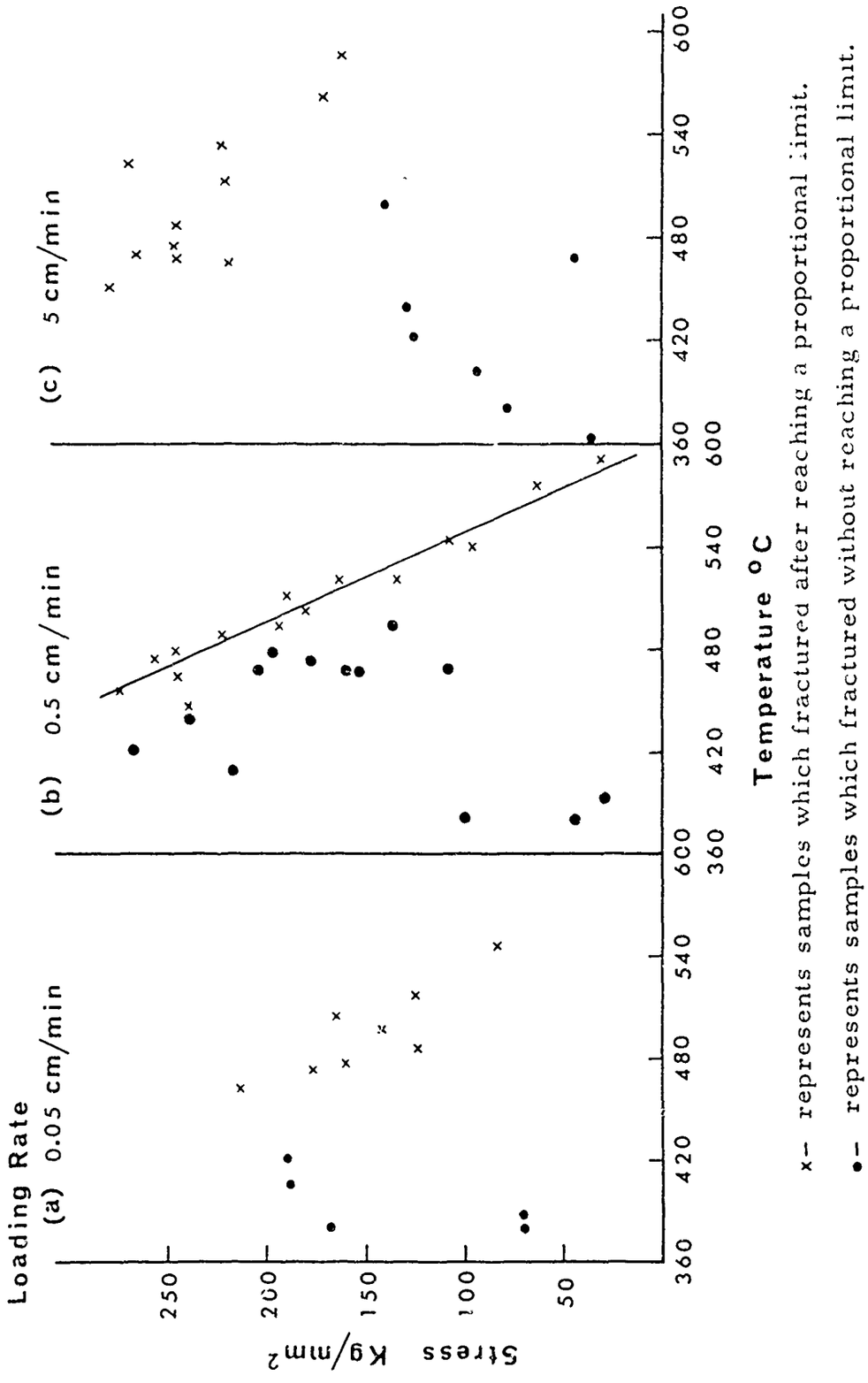

Figure 12. Temperature and loading rate dependence of the tensile strength for treated 4mm to 5mm diameter 7740 borosilicate glass rods.

Effect of Chemisorbed Water on Tensile Strength of 7740 Glass

Chemisorbed water was selected as a possible strength governing mechanism based on the following considerations:

(i) Commercial glass manufacture introduces water into the melt and constitutes an "impurity" of variable concentration.

(ii) Strength measurements of glass usually involve considerable scatter which may be related to water content differences.

(iii) Desorption of absorbed water by thermal treatment could result in surface deterioration in a manner similar to that proposed in earlier studies [10] on the strength-loading rate dependence.

(iv) The desorption of absorbed water may involved rearrangement of the network, the changes being the result of the network collapsing to positions previously occupied by OH^- ions.

(v) Previous work [10] on the effect of water desorption on the strength of glass fibers is variously reported as increasing, decreasing and not affecting strength level.

Several mechanisms have been proposed for water absorption in glasses and a fairly broad review on the subject can be found in Holland's Properties of Glass Surfaces [12]. While it is not within the immediate scope of this study to treat absorption and desorption mechanisms in detail or to determine whether molecular water, hydroxyl groups, or hydrogen bonding is responsible for particular optical absorption bands, sufficient literature references and data are presented as introductory background material.

A synopsis of this review follows: Harrison [12] attributed the infrared absorption bands in the 2.5 to 4.0μ region to OH^- vibrational absorption and suggested that shifts in the absorption band are related to changes in the strength of hydrogen bonding with the principal components of the glass. Glaze [12] proposed that water was present in silicate glasses as molecular H_2O groups.

Moore and McMillan [12] suggested that OH^- groups were associated in the network of the glass modifiers through hydrogen bonding and believed that absorption bands occurring in oxide glasses of low atomic weight arose in the 3μ region due to the OH^- groups. Heaton and Moore [12] studying high molecular weight oxide glasses were unable to decide whether water was present in molecular form or OH^- groups.

Infrared absorption measurements are useful in the determination of the concentration of hydroxyl groups; however, absorption measurements may not be directly used to show whether hydrogen of hydroxyl diffuse through the glass.

After examining several techniques suggested in the literature, it was found necessary to develop a desorption method tailored to the large bulk of 7740 borosilicate glass required for suitable test rods. Crystallization, compositional changes, bubble entrapment, and low level desorption are each eventually overcome by the following technique.

Crushed 7740 borosilicate glass is loaded into a platinum lined depression in a refractory and heat treated at 1600°C under a flowing argon atmosphere for about 12 hours. The desorbed slug is then quenched to room temperature and examined by infrared transmission between 2.5 and 4 microns. The water absorption band is located at about 2.75 microns and represents a 90% reduction in transmittance for undersorbed samples. The extent of desorption afforded by this technique is demonstrated in Figure 13. The desorbed slug is then centerless ground to a 10 cm length 5mm diameter test rod.

Constituent oxide analyses of a sample of 7740 borosilicate glass at 1600°C, under flowing argon, is shown in Table III.

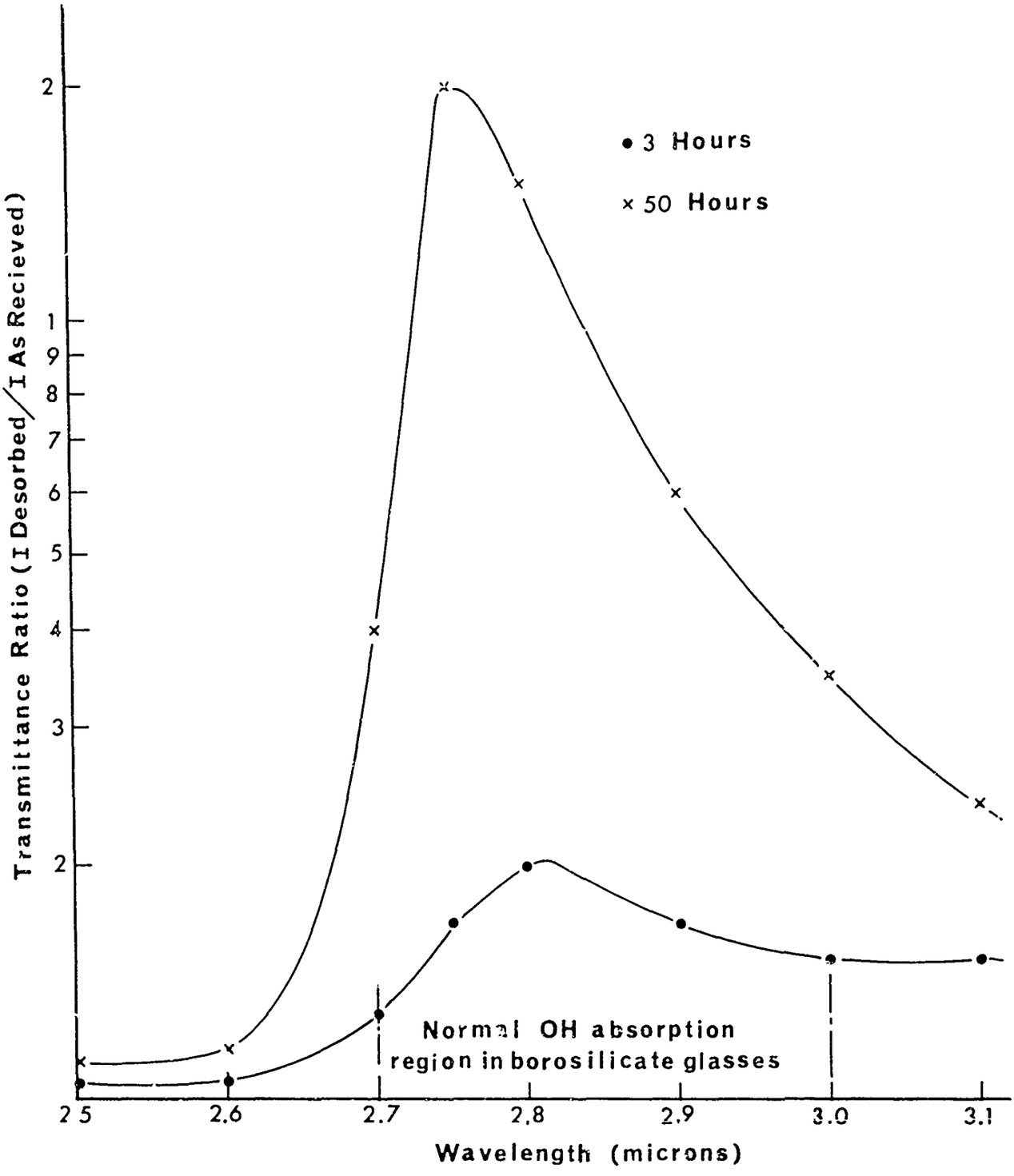

Figure 13. Effect of heat treatment at 1400°C on the water content of 7740 borosilicate glass.

TABLE III

Relative Weight Percentages of Constituent Oxides Found in 7740 Borosilicate Glass Before and After Desorption

Oxide	Starting State	Desorbed State
SiO_2	80.76	82.62
Al_2O_3	2.51	2.50
Na_2O	4.08	2.78
K_2O	0.01	0.009
B_2O_3	12.16	11.83

There is a decrease in the Na_2O content of the desorbed samples. Volatilization of constituents from borosilicate glasses at elevated temperatures was studied by Oldfield and Wright [13]. They report that at temperatures in the vicinity of 1500°C, the weight losses, which are initially large, are influenced after a 20 hour period by the formation of a surface layer. The surface layer is deficient in the volatile constituent and is found to decrease the rate of diffusion of volatiles from the depths of the glass melt.

This may explain why the amount of OH^- removal is observed to approach a maximum with time, showing little improvement with longer treatment times. The prospect of desorbing borosilicate glass without changing composition is not indicated by the studies performed to date. It appears that OH^- free borosilicate glass may require a water free constituent preparation under controlled atmospheres.

Transmission measurements in the water absorption region of "as received", "desorbed", and centerless ground desorbed samples are compared in Figure 14. From Figure 14 it can be concluded that the desorbed state is relatively unaffected by either the centerless grinding process or the 500 hour exposure to atmospheric humidity.

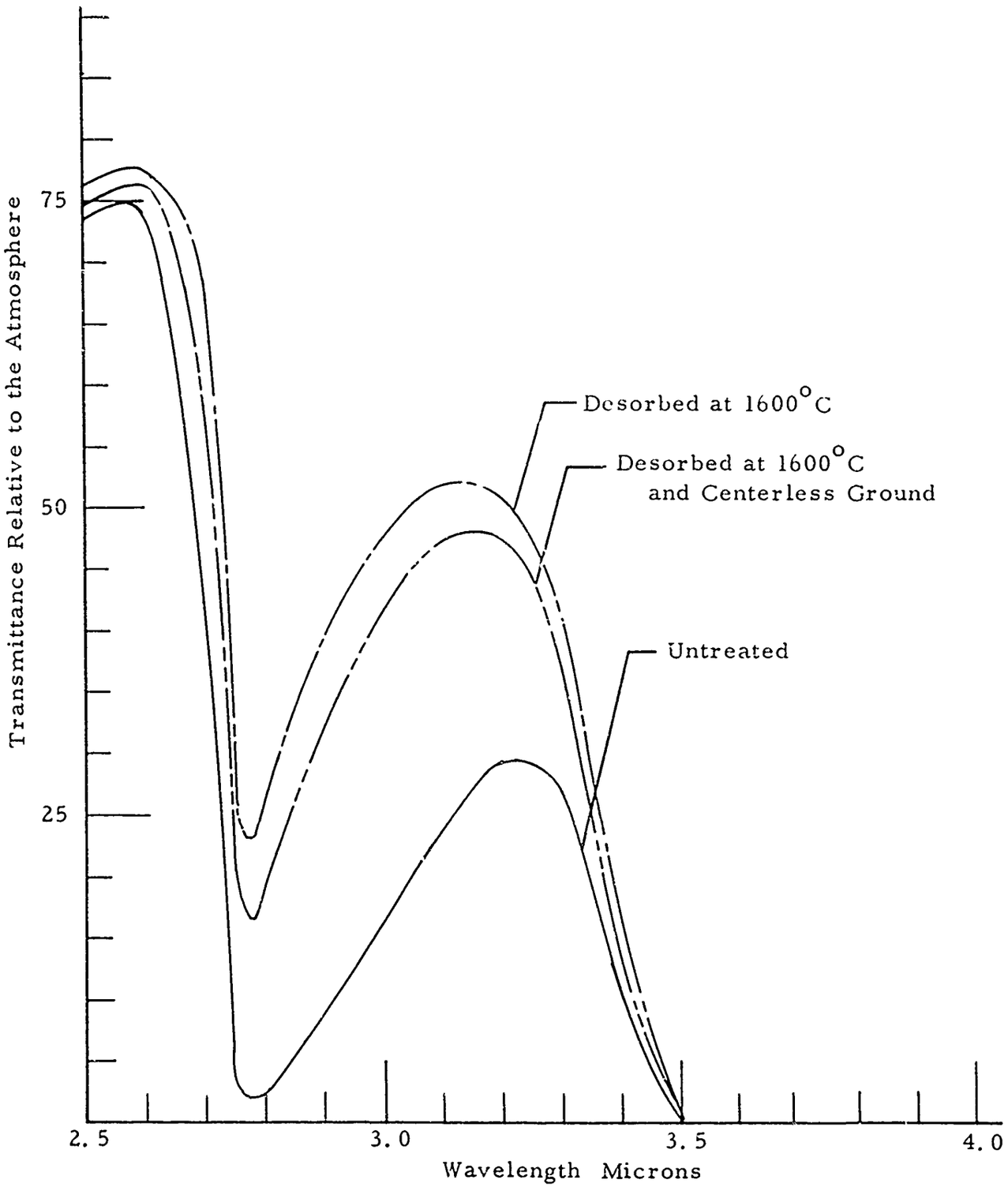

Figure 14. Effect of centerless grinding and atmosphere exposure on desorbed 7740 borosilicate glass.

The effect of chemisorbed water on the temperature dependence of the tensile strength of 7740 borosilicate glass, compared to undesorbed samples, is shown in Figure 15. The desorption process results in an overall reduction in OH^- content of about 50% and, as previously noted, [13] a reduction of sodium oxide content by about 25%. As shown in Figure 15, desorbed samples do not exhibit any obvious strength differences from samples which were treated in an identical manner but not desorbed. In the temperature interval between about 350°and 450°C, where the strength is found to drop off rapidly, the strength of desorbed specimens closely follows the strength temperature dependence of samples not desorbed, suggesting that water content within the range examined here does not appear to affect the strength. The relative insensitivity of the strength-temperature characteristics to both changes in OH^- and Na_2O content is an unexpected result which may be worthy of further examination.

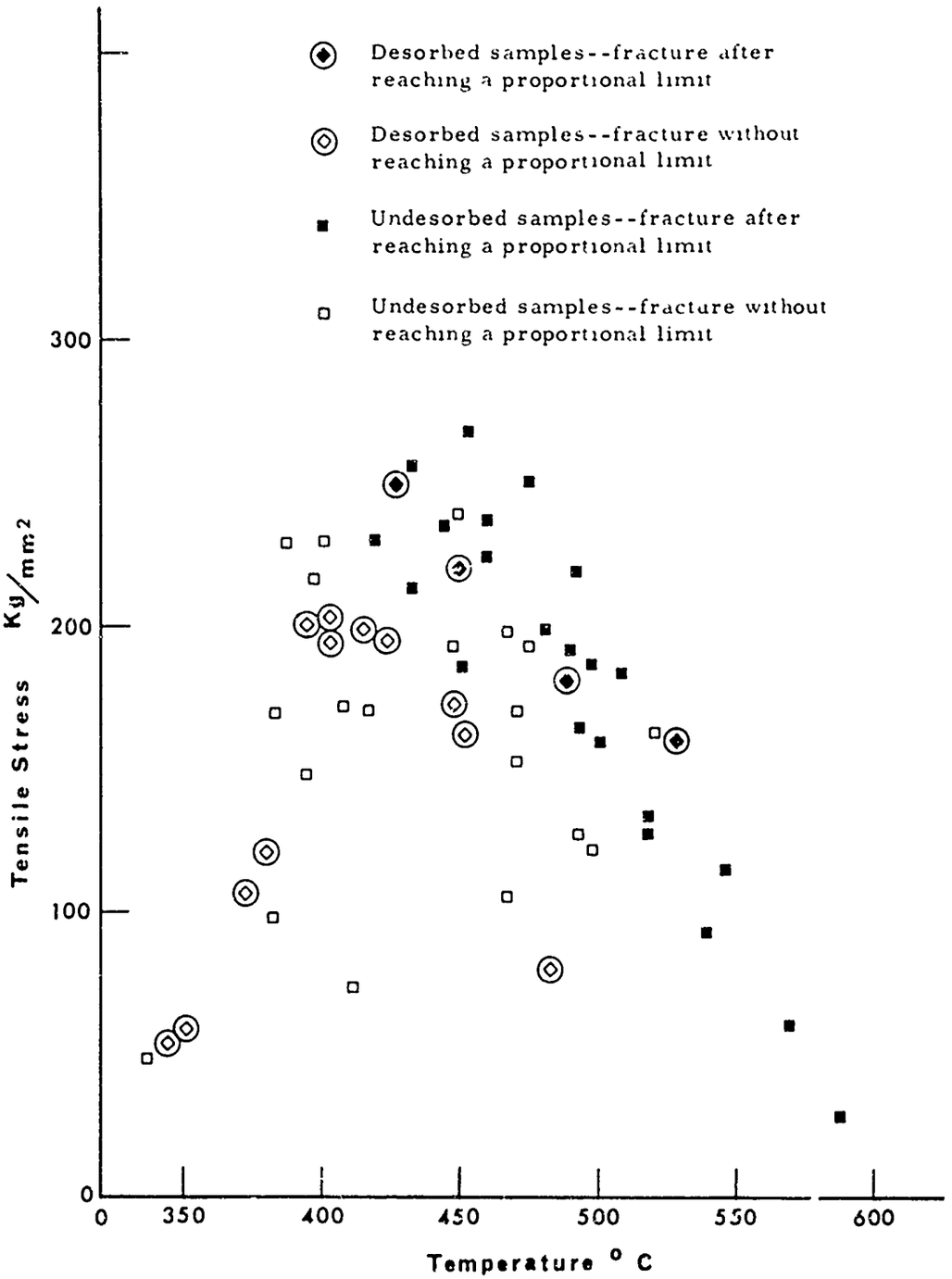

Figure 15. Temperature dependence of the tensile strength of desorbed and undesorbed 7740 borosilicate glass.

C. DISCUSSION

The influence of the coating, coating-core interface, test conditions, and water content on the strength transformation is examined in the previous section. The results of this study suggest that the transformation is more characteristic of the test temperature interval than incidental consequences of test conditions or the coating. In this sense, it appears as a property of state.

In an early treatise, Variation Caused in Heating Curves of Glass by Heat Treatment, [14] A. Q. Tool describes thermal anomalies in the heating curves of glasses. The differences existing between the D. T. A. heating curves of chilled and annealed glasses is considered, by Tool, to confirm the presence of an exothermic effect on cooling and an endothermic effect on heating. Experimental data on "annealed" borosilicate glass is shown graphically in Figure 16.

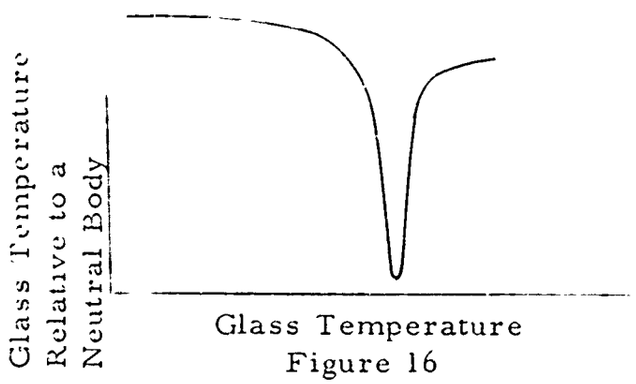

Figure 16

Tool's work on "pyrex" glass suggests that the discontinuity in the heating curve occurred at a temperature corresponding to a viscosity of about 10^{16} poise.

Recently, S. V. Nemilov [15] reports a relationship existing between the free energy of activation of viscous flow and chemical bond energy in glasses and in the article he states: "it is characteristic of the softened state range that the specific heat undergoes an extensive

discontinuity, superficially suggestive of a second order transition". The viscosity interval, wherein the discontinuity in the specific heat occurs, is reported by Nemilov as the 10^{16} - 10^{18} poises (softened state range). The 10^{16} - 10^{18} poises viscosity range for 7740 glass corresponds to a temperature interval of about 400°to 500°C. The strength transformation observed in 7740 and 7720, as previously noted, occurs at different temperatures corresponding to the same viscosity, about 10^{17} poises.

In this connection Lillie [16] reports that when a glass is at a temperature corresponding to an equilibrium viscosity of about 10^{16} poises, a change in load results in an immediate "elastico-viscous elongation", but after some time the elongation curve returns to the original state. A later study [17] discusses viscosity time anomalies peculiar to borosilicate glasses. Unlike silica glasses, borosilicate glasses are found to require considerable time to reach stabilization in the viscosity range above 10^{13} poises. The authors suggest, as a possible explanation, that the increased time is associated with a change in boron coordination from 3 coordinated, as in B_2O_3, to four coordinated. They further suggest sodium ions migrate to positions where they are surrounded by oxygen atoms belonging to the BO_4 tetrahedron. The relation between sodium content and boron atom coordination is well known [10]. Radial distribution studies of borosilicate glasses for various amounts of sodium oxide addition are interpreted as involving a change in coordination from three coordinated to four coordinated occurring at certain concentrations. These results suggest two possible models consistent with the strength-temperature transformation. First, a thermally induced change in coordination of the boron atom in borosilicate glass may result in a generally weaker structure and second, at high viscosities (near 10^{16} - 10^{18} poises) flaw free-protected borosilicate glass can sustain sufficient stress to produce migration of sodium ions resulting in a change in B-O coordination. Both models are subject to some degree of verification by experiments which explore the relationships of radial distribution peaks with temperature and stress--a possible fruitful area for further work.

III. ELECTRICAL PROPERTIES OF 7740 BOROSILICATE GLASS

Since the method of strength measurement used in this work gives values representative of the intrinsic strength of glass, it is desirable to correlate the strength data with other physical properties. Of particular interest are electrical properties which in glass have a closer correlation with mechanical properties than is the case with most materials. This is largely the result of the fact that glass acts much like an electrolyte; that is, the current is carried by ions. Since ionic charge transport involves the transport of considerable mass, as compared to electronic conduction, it is reasonable to expect a close correlation between electrical and mechanical properties. The connection between the two is perhaps most strikingly apparent in the observed relation between resistivity and viscosity. It has been shown, for instance, that for soda-lime glass the following relation holds between the resistivity ρ and η over a large temperature range.

$$\rho = A \eta^{1/4}$$

where A is a constant. Since both the resistivity and viscosity depend exponentially on activation energies, an expression of this type shows that the activation energy for ion migration and the activation energy for the flow process are related. Although the relation between viscosity and resistivity is not as simple for most glasses as the one given above, the basic form remains about the same. As pointed out by Stanworth, other mechanical properties can likewise be correlated with electrical properties though not perhaps in the concise form used in this example. [18]

In the context of this work, the possibility of establishing a relation between electrical and mechanical properties may provide a potential tool for investigating the strength-temperature transformation discussed in Section II. Recall that, quite generally, there are two possible sources for the strength-temperature transformation. It could be (i) a characteristic of the composite structure or (ii) a property of the bulk material. The characteristics of the composite structure, examined and discussed in the previous section, suggest that a bulk property change is the more probable cause of the

strength transformation. To further examine this possibility, it is desirable to investigate the behaviour of other bulk physical properties in this temperature range. Electrical methods are well suited for this in that they are comparatively simple and there is ample reason to believe that a change in the inherent strength of glass should be reflected in the electrical properties. While, as has been noted, a connection between electrical and mechanical properties can be expected in glass, interpretation of electrical data is difficult because of the disordered aspects of the glassy state.

Both the dielectric constant and the electrical conductivity can be regarded as depending on some form of activation energy which must be overcome before polarization or charge transport can occur. In a crystal, matters are simplified considerably by the fact that, to a good approximation usually, polarization due to the ionic lattice and to the free electrons can be treated separately, with negligible contribution from ionic migration. Conceptually, the situation is simpler still for charge transport in a crystal, for here lattice contributions can be ignored altogether. In a crystal, one has the additional advantage that the material can be regarded as homogeneous and isotropic. Two relaxation times, one for the lattice and another for the conduction electrons, are then usually adequate for a discussion of both transport and polarization.

The situation in the glass is considerably more complicated. First, the terms homogeneity and isotropy must be applied with caution in the case of glasses. The view first advanced by Zachariasen, that glass constitutes a random network, is now widely accepted. On a microscopic, but not on an atomic, scale glass may be regarded as both homogeneous and isotropic in the sense that its microscopic composition and properties are independent of position and direction. On the atomic scale, glass appears to have a wide range of structures and compositions which must be regarded as some statistical distribution and this fact has greatly hampered theoretical predictions of its electrical

properties.

In the case of crystals, one may make relatively direct and unambiguous measurements (with x-ray diffraction techniques) on the atomic appearance of the crystal. Thus the electrical environment of a charge carrier is known, and it is practical to compute the carrier's response to an externally applied field.

Analogous measurements in the case of glasses are in an embryonic stage. Scattering studies yield, at best, only information on some "average" environment of charge carriers. This information is, in general, inadequate for rigorous predictions of electrical behavior for much the same reason that the mean of a set of data fails to specify the data's spread. Many qualitative models are available for the distribution and nature of voids in glasses which "explain" conduction, but to date all have little factual support.

Similarly, in the case of crystals, processes such as polarization often are associated with some characteristic response time (relaxation time) which is in turn related to the mass of the atom and stiffness of the lattice. The variation of polarization with frequency is usually a simple function of this relaxation time. As might be expected from the statistical nature of glass, and in fact supported by our experimental work and by the work of others, no such simple relaxation time approach applies to glass. Rather, in order to explain the observed behavior of quantities like dielectric constant and resistivity on the basis of plausible mechanisms, it is necessary to postulate a spectrum of relaxation times. However, the theoretical machinery for deducing such a spectrum from independent measurements does not yet exist and it is not possible to conclusively determine whether the "plausible" mechanisms are, in fact, responsible for the observed behavior. The above discussion points out the tremendous difficulties inherent in a theoretical approach to the study of glass at the present time.

A. DIELECTRIC CONSTANT AND LOSS TANGENT MEASUREMENTS

Since the dielectric properties of glass reflect the effects of ionic displacement and, in some cases, slight network rearrangements, measurement of the dielectric constant and loss tangent in the temperature interval of the strength transformation should indicate the role of these mechanisms in the phenomena. A description of these measurements and results obtained are given in what follows.

It is well known that glasses exhibit both capacitive and resistive behavior, and a given specimen may be represented at any fixed frequency by the equivalent circuit of Figure 17. This simplification

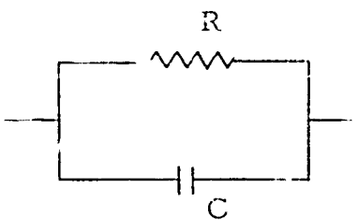

Figure 17

does not fully specify the overall electrical properties of glass, since C and possibly R vary with frequency. Rather than measure R and C, it is customary to measure the dielectric constant, K, and the loss tangent

$$\tan \delta = \frac{\text{reactance of specimen}}{\text{resistance of specimen}} = \frac{1}{\omega \epsilon_0 K \rho}$$

where ρ is the resistivity of the specimen. From a knowledge of tan δ and K, it is therefore possible to compute ρ.

General Radio Capacitance Bridges, Types 716C and 716CSL, together cover the frequency range 30 Hz to 3 MHz. These bridges meet American Society of Testing and Materials specifications. They do have one drawback for this research, however, in that they are intended for use with rather good dielectrics; poor dielectrics such as the glasses studied in this program are ordinarily of little interest.

Study of the literature reveals no information on K and tan δ in the 400°to 600°C temperature interval. For this reason measurements are initiated near room temperature, where data is available for verification of the technique, and proceed up in temperature to the bridge limits.

The specimens are in the form of square plates 3" X 3" X 3/32" cut from a single sheet of plate glass in order to reduce the possibility of varying chemical composition. A two terminal measurement was used rather than the common guarded electrode or micrometer electrode schemes since these are impractical at high temperatures. The electrodes are of chemically deposited platinum since this material neither oxidizes nor diffuses into glass at the temperatures used. The furnace temperature is regulated to $\pm$ 5°C.

The expected capacitance of such a plate is about 100 pf at 300°C which is not very large in comparison to the stray capacitances present. While it is possible to work with multiplate capacitors, any benefits accrued from such an arrangement would be counteracted by the difficulties of maintaining plate alignment and of computing the edge and ground capacitances. Therefore, single plates are used for which very good correction formulas are available. The computational methods used are those of ASTM D-150.

The results of the dielectric constant and loss tangent measurements are shown in Figures 18 and 19. Both of these variables exhibit roughly the same qualitative behavior: a steep non-exponential rise with increasing temperature and an approximately logarithmic shift with frequency. The above data is taken by slowly cooling the specimen from 600°C (where, there is reason to believe, soaking for two hours destroys all previous thermal history) to the lower test temperature. The measurements are then made by raising the temperature slowly and remaining at each desired temperature until K and tan δ are constant over a half hour period. This procedure, therefore, attempts to produce equilibrium conditions in the specimen, though the term must be used cautiously

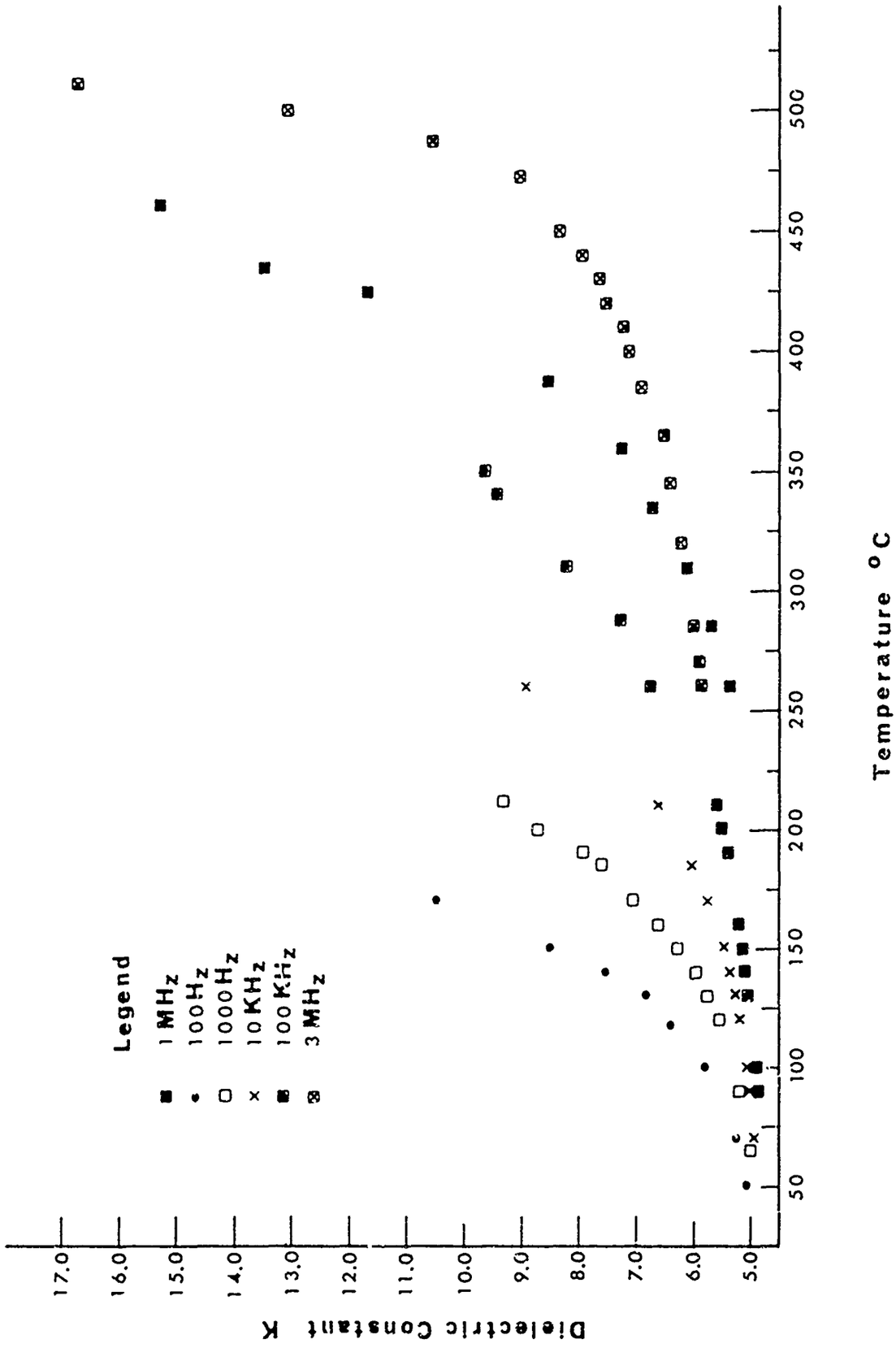

Figure 18. Temperature dependence of dielectric constant in 7740 borosilicate glass.

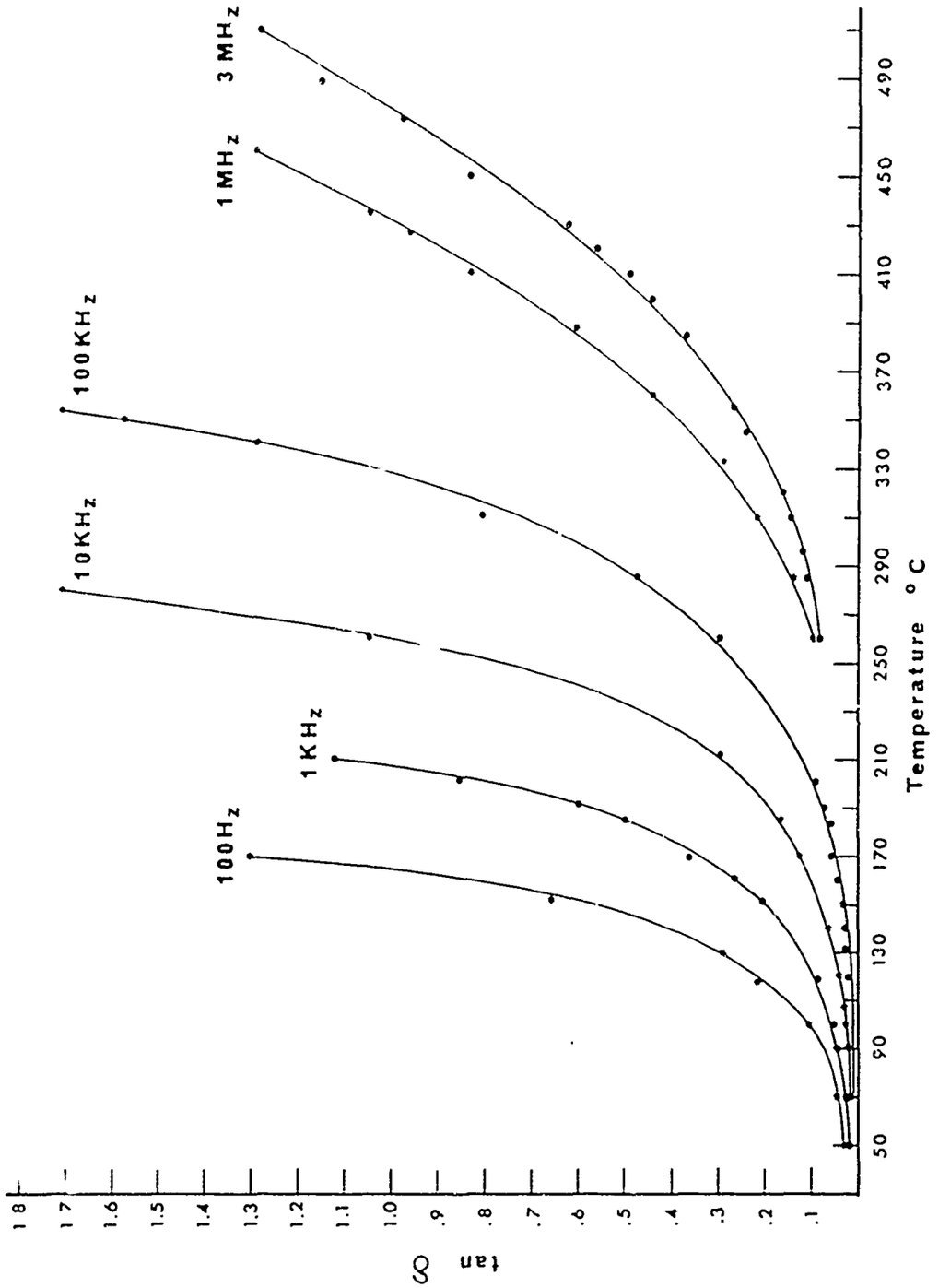

Figure 19. Loss tangent vs. temperature for 7740 borosilicate glass.

since, as the work on electrical conductivity shows, equilibrating processes with extremely long time constants exist in glass.

The temperature interval of interest to this investigation (400°C to 600°C) is found to limit the number of variables that can be examined with the commercial apparatus employed. The values of loss tangent and dielectric constant, in this temperature range, rapidly exceed the bridge capacity at lower frequencies and therefore, while Figures 18 and 19 do provide information not previously available, sufficient range of variables can not be provided to determine any resonance behavior possibly occurring near 450°C. It would, of course, be desirable to determine both the dielectric constant and tan δ at higher temperatures but to do so would require the design of a Schering bridge (the type used in the General Radio units) specifically intended for the range of variables found in this glass. This idea is not without merit but would involve a considerable amount of development and testing. Although possible resonance effects could not be examined, fixed frequency studies offer an alternate approach to examining the effects of a network transformation. Quenching is widely known [19] to temporarily 'freeze-in' the more open structure present at high temperatures. Since the conductivity increases with temperature it is to be expected that tan δ should be higher (at least initially) for a quenched sample. The results of such a quenching experiment are presented in Figure 20 and bear out this conclusion; the effect, however, is surprisingly small. In the work (to be discussed) on electrical conductivity, quenching is found to produce drastic changes in results.

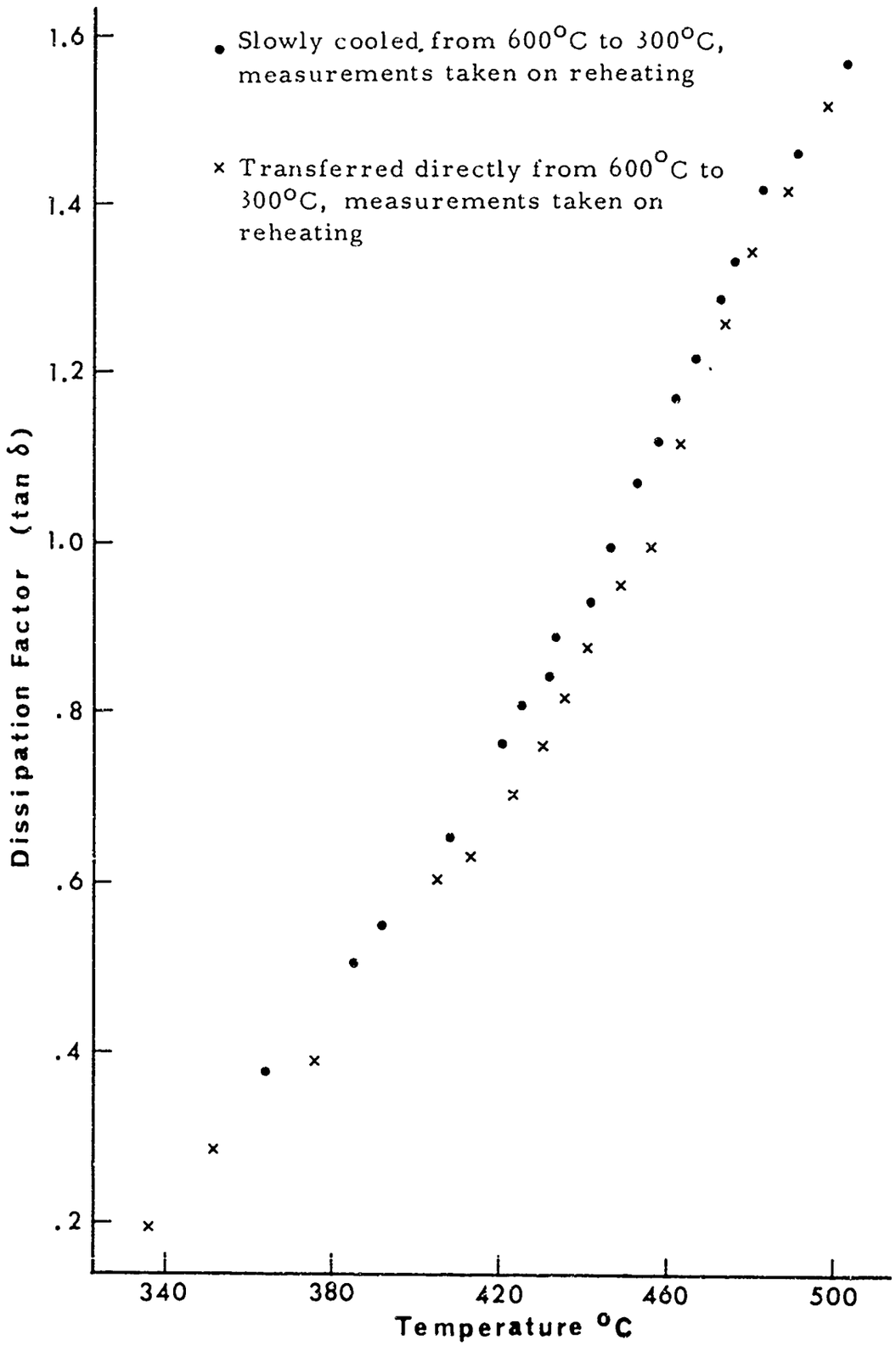

Figure 20. Effect of thermal history on the temperature dependence of dissipation factor of 7740 borosilicate glass.

B. ELECTRICAL CONDUCTIVITY MEASUREMENTS

Electrical conductivity studies offer the same potential in revealing changes in the network as the dielectric constant and loss tangent while permitting considerably more latitude in test variables for the temperature range of interest.

If the resistivity predominates over the dielectric constant, (i. e. if $R > 1/\omega C$), the capacitance may be ignored and ρ measured by simple means. However, if the capacitance is comparable to the resistance, one requires a means for isolating the current components due to R and C, which are in phase quadrature. A rough projection of the dielectric constant results suggests that the former assumption is probably applicable (an independent check of this assumption was later performed). Note that this is not tantamount to assuming that the D. C. results will be obtained; the resistivity includes losses due specifically to the use of A. C. rather than D. C. current. The A. C. losses, however, must contain the D. C. losses as a component. One may thus say quite generally that $\rho_{AC} \leq \rho_{DC}$.

The arrangement first used is shown in Figure 21(a). Resistor R_c is placed in series with the specimen and the potential across it measured with a simple peak reading voltmeter consisting of a rectifier, filter, and D. C. electrometer (portion to right of dotted line). This circuit was used for some initial low voltage measurements but was ultimately abandoned for two reasons. First, in order to obtain adequate sensitivity, R_c had to be comparable to the specimen resistance. This caused the actual potential applied to specimen to vary considerably as its resistance changes. Second, the A. C. voltage had to be applied for about twenty seconds in order to make a measurement. These characteristics are relatively unimportant at low voltages where glass is thought to be ohmic, but become significant at higher potential gradients where glass is widely held to be nonohmic. In this case it is necessary to control the applied potential. Further, at, say, 200 volts/cm the power dissipated in the specimen can run to several watts. Thus a satisfactory measuring technique should make provision for rapid determination of resistance.

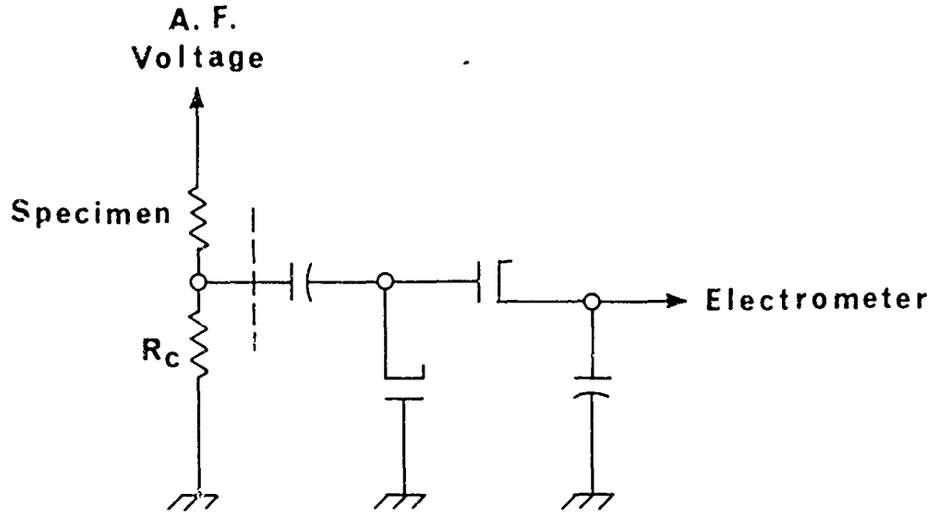

(a)

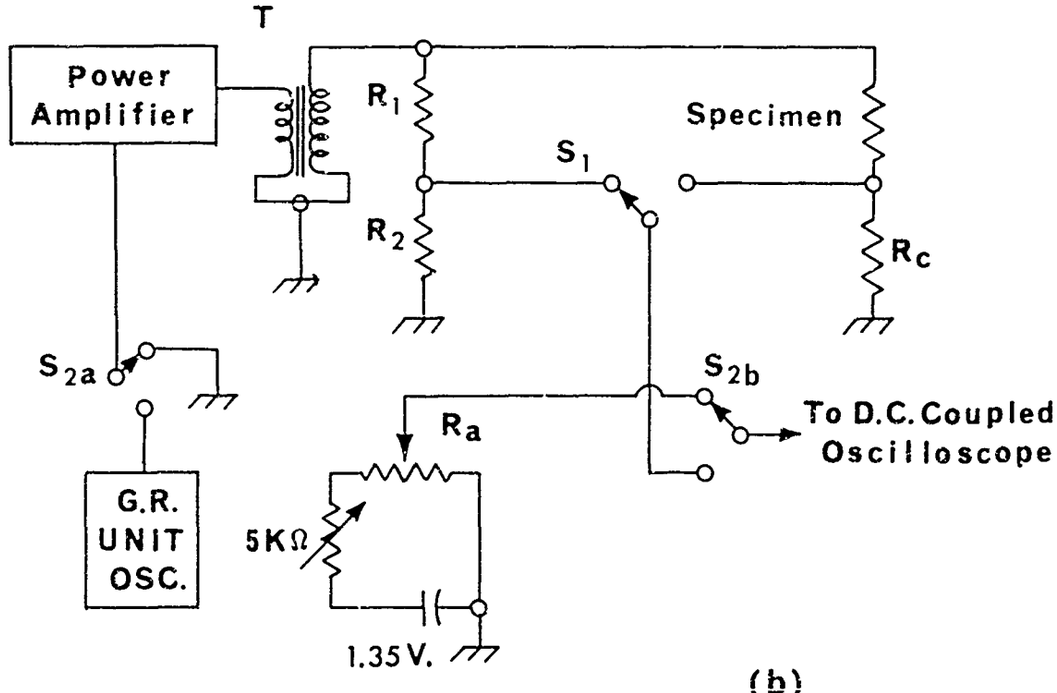

(b)

Figure 21. Electrical resistivity measurement circuits.

The scheme ultimately used proved reasonably satisfactory. Figure 21(b). This is a comparison technique where the A. C. potentials involved are compared to an accurate D. C. reference voltage. The 1.35 volt cell, R_a, and the 5 Kohm potentiometer constitute the D. C. standard. The 5 Kohm potentiometer is adjusted so that 1.000 volt appears across R_a. R_a is a ten-turn potentiometer, linear to 0.1%, equipped with a turns counting dial so that the potential appearing at its tap may be read directly to 1 millivolt. It is normally connected to the oscilloscope through relay contacts S_{2b}. This relay is controlled by a key (not shown), which also connects the oscillator and power amplifier when tapped.

The signal from the amplifier is stepped up by transformer T and applied to the series arms R_1 - R_2, and R_c, and the specimen. R_1 and R_2 are chosen so that slightly less than one volt appears across R_2 when the transformer voltage has the desired value (either 100 or 200 volts in these experiments). With S_1 in the position shown, this calibrating voltage is set up on R_a, and by tapping the key and adjusting the oscillator output, equality of the two voltages may be quickly established.

The voltage across R_c is then determined by switching S_1 and adjusting R_a until its voltage, V_{Ra}, equals the peak voltage across R_c. R_c is chosen to be $\leq$ 1% of the specimen resistance so that the voltage actually applied varies only slightly with its resistance changes. The resistance of the specimen is then computed from

$$R = R_c \frac{V_{applied} - V_{Ra}}{V_{Ra}} \qquad (13)$$

Note that the key need only be tapped briefly so that specimen heating is avoided.

The samples were short rods, about 1 cm long by 1 cm in diameter, with platinized ends. They were held in a spring-loaded holder which pressed platinum foil contacts against their ends which avoided possible contamination.

Since glass is nonohmic at high potential gradients, two values of A. C. voltage were used in measuring the temperature dependence of resistivity for various frequencies. The results for 100 V/cm and 200 V/cm are shown in Figures 22 and 23. In both cases, the samples were held at 600°C for four hours prior to the start of a run. This was considered adequate for achieving equilibrium conditions since tests showed a 1% resistivity change in 24 hours at 600°C. The temperature was then reduced in 25°C intervals, held constant for at least two hours prior to test, and several measurements of resistance performed over a half hour period. It was found that this procedure produced no changes in resistance over the (half hour) test period.

At low frequencies, and particularly at high temperatures, the usual linear behavior of log ρ vs. 1/T is observed. In this region the results shown in Figures 22 and 23 follow the Rasch and Hinrichsen relation derived by considering only conduction losses

$$\log \rho = A + \frac{B}{T} \qquad (14)$$

where T is the absolute temperature. As the frequency is increased, however, there is a clear trend downward in the log ρ curves which becomes quite evident at 30 KHz. This behavior is similar to that observed by Robinson [20] in resistivity measurements on soda-lime glass, "pyrex", and quartz. While Robinson's study did not provide very much range in frequency or temperature, one aspect of his results may be important to this investigation. The temperature at which the deviation from the linear behavior is observed is lower for the soda lime glass and higher for the quartz sample, internally consistent with the relative conductivities of soda-lime glass, "pyrex", and fused quartz, if a concentration effect is involved.

The effect of different potential gradients, shown in Figures 22 and 23, is quite small for low frequencies: the curves for frequencies up to 3 KHz coincide. At 30 KHz the curve for 200 V/cm is above the 100 V/cm curve at low temperatures and below at high temperatures.

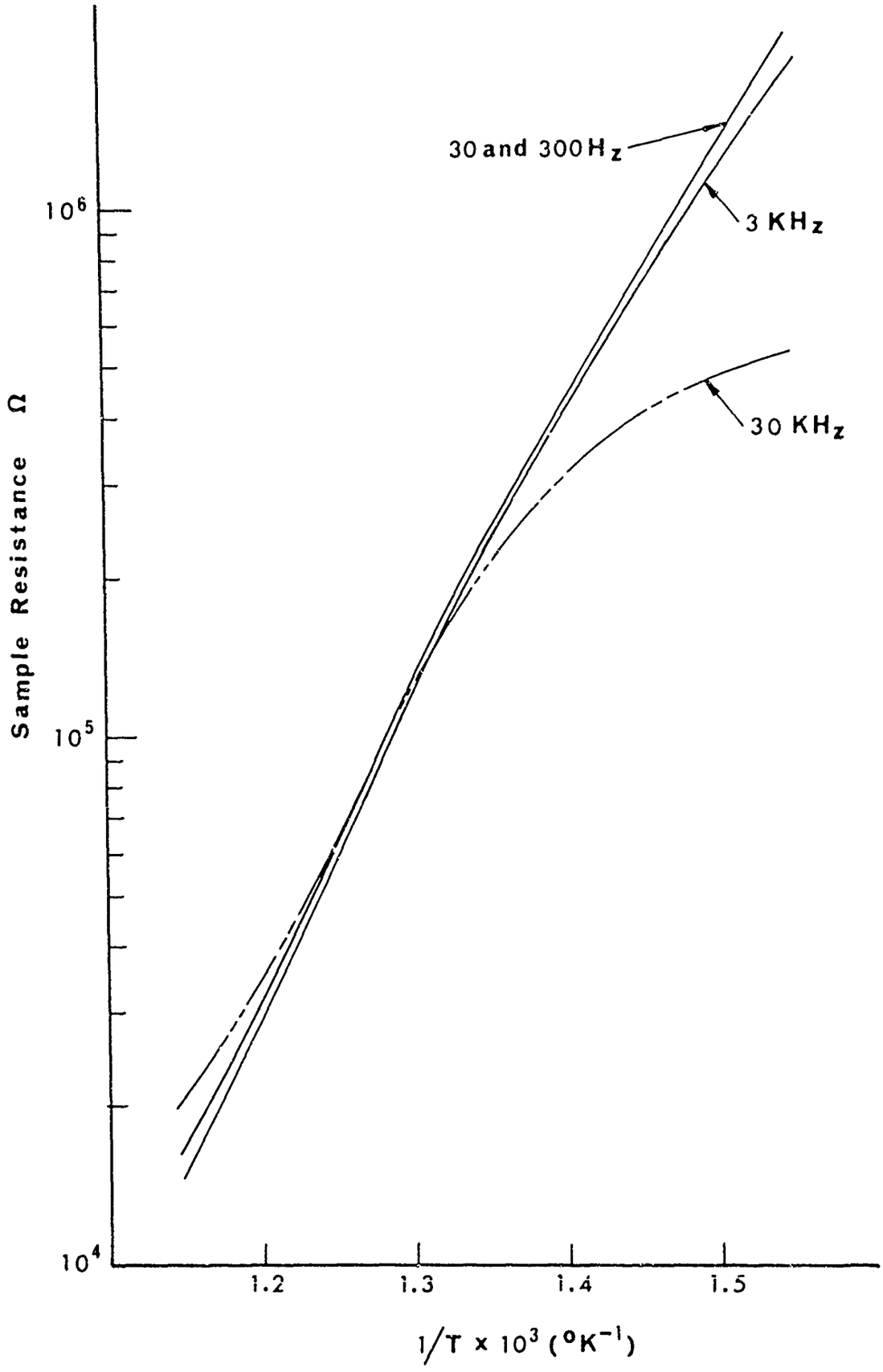

Figure 22. Temperature dependence of electrical conductivity of 7740 borosilicate glass at field strength of 100 V/cm.

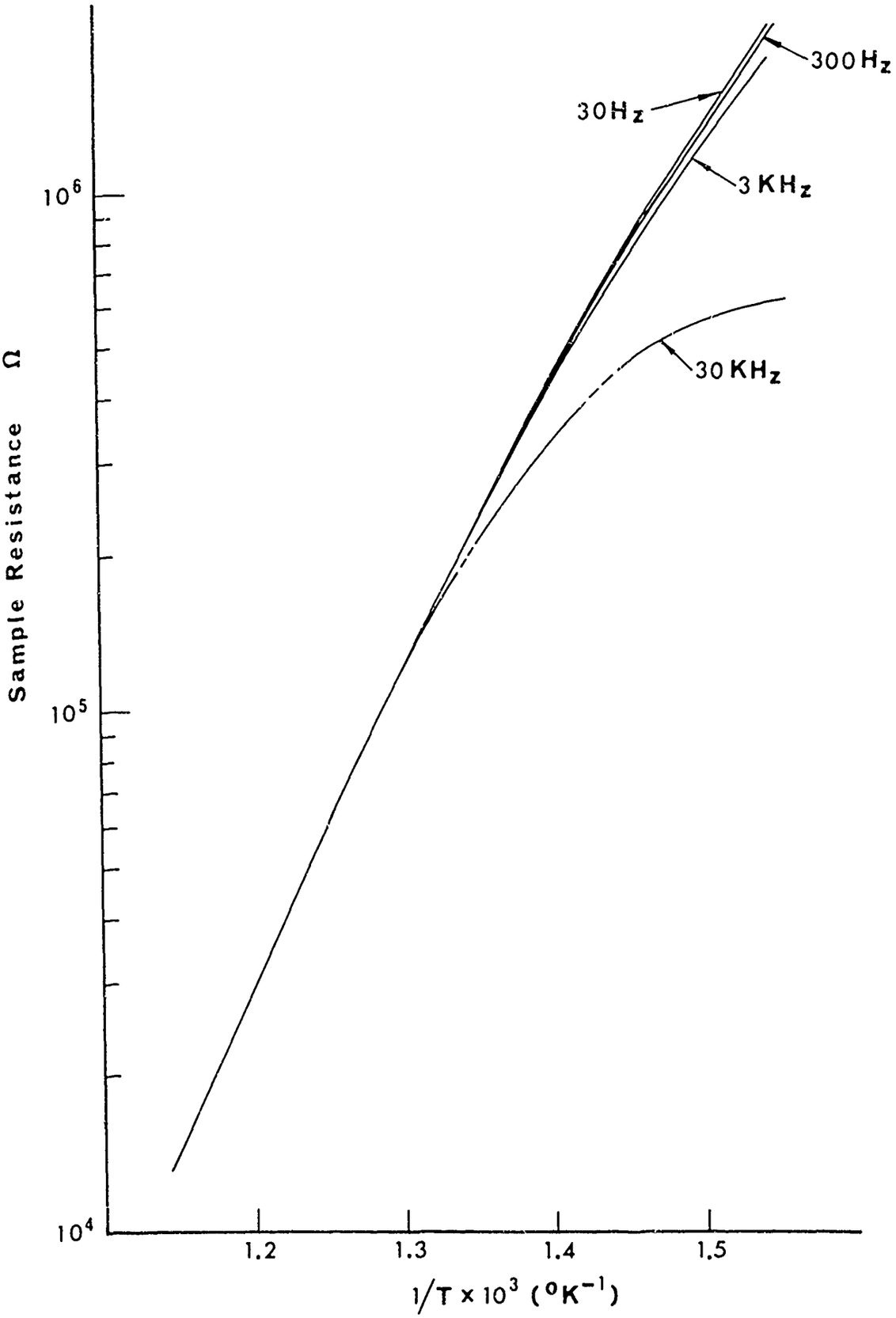

Figure 23. Temperature dependence of electrical conductivity of 7740 borosilicate glass at field strength of 200 V/cm.

While it is premature to comment on this effect, it does appear to be contrary to Poole's empirical relation for D. C. voltage gradients

$$\log \rho = \text{const} - \rho|E| \qquad (15)$$

where ρ is a constant and E is the electric field.

To eliminate the possibility that the downward shift observed at high frequencies is the result of the "slow cool" heat treatment used in the above measurements, specimens were quenched from 600°C to two different temperatures and the resistance measured against time. The results for samples quenched to 500°C and 425°C are shown in Figures 24 and 25. Note that, in accordance with the previous results, there is no appreciable difference in resistance at high and low frequencies for the sample quenched to 500°C while there is a significant difference for the sample quenched to 425°C. It is also worthwhile to note that in the later case time at temperature has a more pronounced effect on the low frequency results; the final to initial resistance ratio is about 1.45 for 3 KHz and lower frequencies while the same ratio is 1.25 for 30 KHz. This suggests that the low frequency resistance, which for discussion purposes can be taken to be the D. C. component of resistance, is more affected by structure homogenization due to annealing. Since the D. C. component would be likewise affected in the high frequency measurements, it appears that the high frequency loss mechanism responsible for the downward trend in log ρ is not particularly structure sensitive but results, instead, from dynamic interactions.

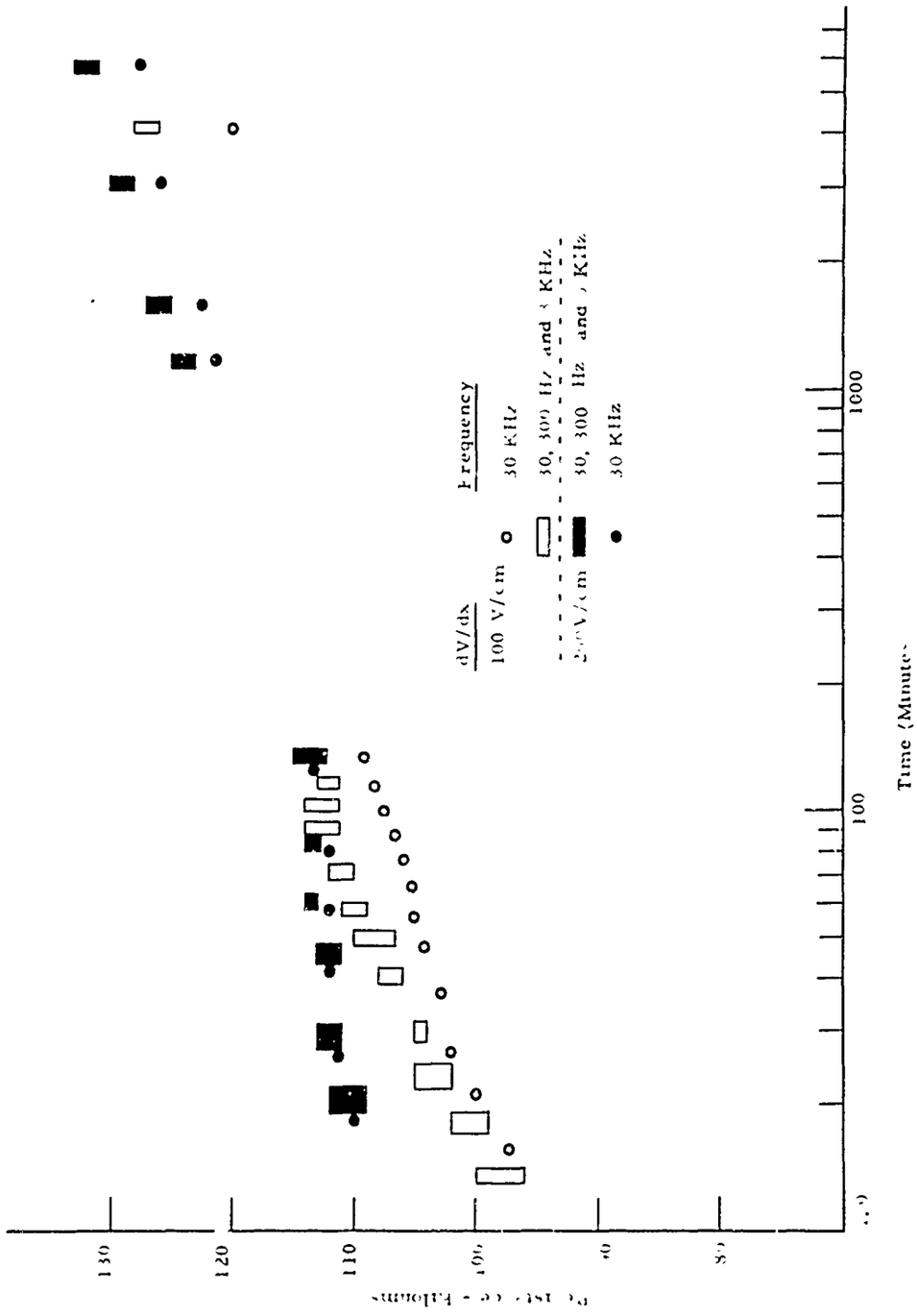

Figure 24. Resistance vs. time for 7740 sample rapidly cooled from 600°C to 500°C.

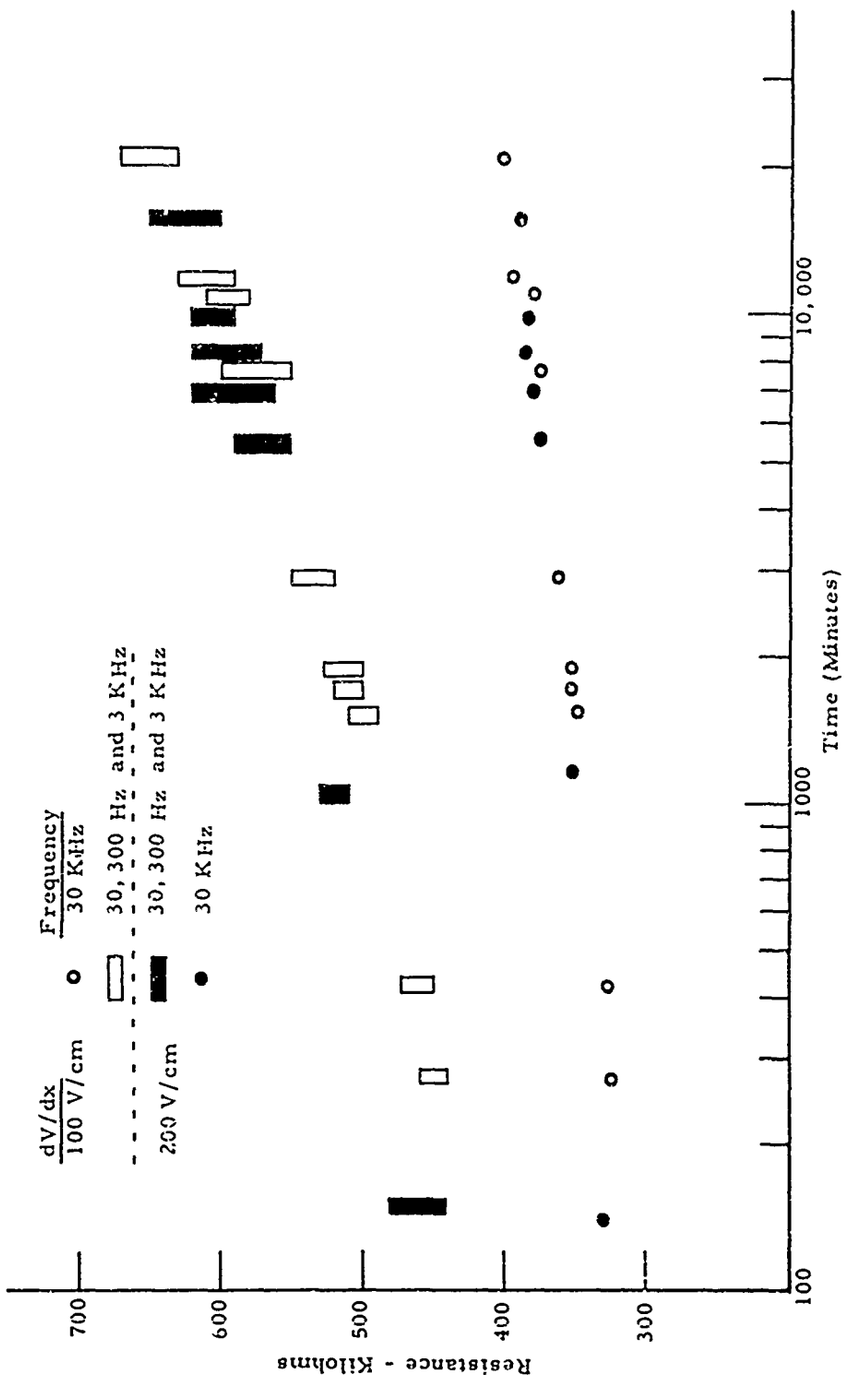

Figure 25. Resistance vs. time for 7740 sample rapidly cooled from 600°C to 425°C.

C. DISCUSSION AND FURTHER EXPERIMENTS

The final point of the previous section--viz, the apparent insensitivity of frequency dependent losses to structure--has relevance to the question as to why nothing suggestive of a structural transition was observed in either the dielectric constant or conductivity measurements which together cover the range of the strength-temperature transition. The reason for this probably lies in the nature of the losses represented by tan δ and the macroscopic resistivity ρ. It is important to note that in the definition of the loss tangent

$$\tan \delta = \frac{1}{\omega \epsilon_o K \rho} \tag{16}$$

ρ is defined phenomenologically rather than being ascribed to any particular source. That is, for a specimen of unit length and cross-section

$$\rho = \frac{V^2}{P} \tag{17}$$

where V is the r. m. s. value of the applied potential and P the rate of energy loss in the specimen.

Now, since a number of loss mechanisms are probably active, each with its own resistivity contribution ρ_i, the measured ρ is given by

$$\frac{1}{\rho} = \sum \frac{1}{\rho_i} \tag{18}$$

which, when substituted in the equation for loss tangent, gives

$$\tan \delta = \sum (\tan \delta)_i \tag{19}$$

The individual contributions to tan δ are thus directly additive. In the context of this work it then becomes important to determine which of the individual loss mechanisms can be expected to be structure sensitive.

The two principal losses to be considered are: vibrational and migrational. The vibration losses result from damped forced oscillations of all ions within the glass. The natural frequency of any ion, whether network former, network modifier, or oxygen, depends upon its mass and stiffness. This does not lead to a few well defined resonances, unfortunately, since the stiffness is dependent upon the immediate surroundings of the ion. The surroundings are so variable in glass that the vibration spectrum covers an enormous continuous range. Further, the spectrum shifts downwards with increasing temperature to encompass the range of audible and low radio frequencies.

The migrational losses are of two types, both of which are due to motions of the sodium ion. The first of these is the conduction loss, resulting from collisions with the network during motion over comparatively great distances. The ρ appropriate to this process is simply the ρ found in d. c. conductivity measurements.

The second migrational loss is the dipole relaxation loss. This loss involves sodium transport over relatively low potential barriers and comparatively short distances. Picturesquely, one may think of small closed voids within which entrapped alkali ions may slosh about under the influence of an applied field. Thus as far as these losses are concerned, the effect of an external field is to produce a slight displacement of the center of charge equivalent to polarization (in the capacitive sense). Indeed, the loss mechanisms is identical to that of an ordinary polar molecule excited near its natural frequency and the loss is given by the usual Debye expression

$$(\tan \delta)_{\text{dipole relaxation}} = \text{const} \frac{\omega \tau}{1 + \omega^2 \tau^2} \qquad (20)$$

Actually, as is usual with glass, a spectrum of relaxation times is involved so that the simple maximum expected from this expression is not actually observed.

While the vibrational losses are obviously influenced by structure

their nature tends to produce an averaging effect which probably washes out small and subtle changes. Hence, the fact that no dramatic behavior is observed in the measurements may simply indicate that the losses dominating in this frequency range are not sensitive to the structure of interest.

In the light of the above ideas, the loss tangent data was carefully re-examined for possible small anomalies. In the 3 MHz data, a possible abrupt change in slope did occur at about 430°C. This portion of the experiment was then carefully re-run in order to fill in the region in detail (Figure 26) and determine if scatter could account for the original appearance. The dots represent the first run with a slow cooled specimen. There does appear to be a slight peak at 430°C accompanied by a change in slope; the appearance of the data at lower temperatures indicates little scatter. The specimen was then held at this temperature for several hours and the measurements repeated. After this the peak appeared to have annealed out.

The work to date indicates that, in the temperature range of interest, those components of the electrical resistivity of glass which are known to be sensitive to structure are easily obscured. The techniques employed do readily show the effect of such gross structure modifiers as quenching and there is some evidence that more subtle structural changes are affecting the resistivity. However, with the A. C. methods used, it was not possible to go much beyond what has been done and it appears that one might do well to employ D. C. methods. Measurement of D. C. conductivity is ordinarily avoided due to the presence of the anomalous absorption current which manifests itself in a slow decrease in the specimen current over a period of several minutes. This raises the problem of deciding which current should be taken as representative of the resistance. The question is not simple; although the current is known to be due to alkali migration, the effect does not yet have a complete theoretical explanation. The most recent thinking due to Sutton [21] indicates that the initial current is the fundamental quantity.

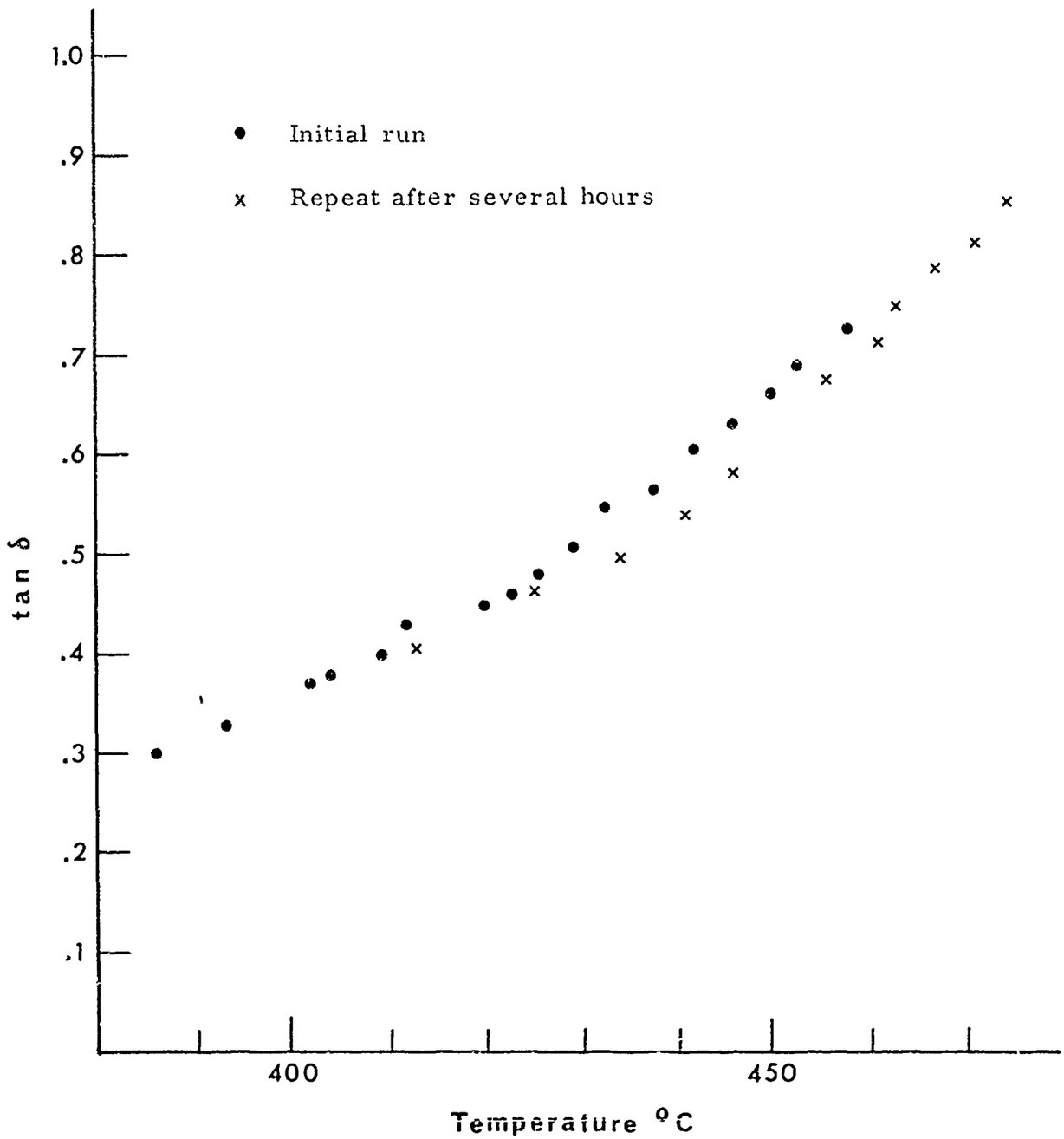

Figure 26. Re-run of loss tangent measurements. Note apparent change of slope near 430°C.

From the viewpoint of this study, the qualitative aspects of Sutton's explanation are sufficiently suggestive of application. Briefly, voids within the glass are held to be of three types: (1) voids and channels possessing essentially continuous communication over the length of the specimen, (2), voids possessing only lateral communication with the lengthwise channels and, (3) blind voids. Under the applications of an external field, all available alkali ions begin to migrate in the preferred direction so that the initial current is high. The current then decreases due to three influences: (a), the ions in the types (2) and (3) voids are effectively removed from the carrier stream, (b), as the type (1) ions arrive at the cathode they are removed from the stream, and (c), the buildup of ions at the cathode reduces the magnitude of the internal field so that the drift velocity is reduced. The current does not decline to zero, however, because under the influence of thermal excitation the ions trapped in type (2) voids gradually work their way into the lengthwise channels to provide a current which is essentially constant over long periods.

If this view is correct, the anomalous absorption current (especially its early time development) should constitute an analytical probe of internal structure which eliminates the screening effects of the vibration spectrum. In particular, its initial value should give information on both short and long range structure while its later values are indicative of long range structure alone. The feasibility and implementation of such an approach are presently under study.

IV. LOW MELTING POINT GLASSES

The sulfide program is devoted to exploring glass systems suitable for room temperature high strength composite structures. The main requirement in this case is that the coating remain relatively fluid down to room temperature and below. In addition, experience with the high temperature (borosilicate)glasses indicates, perhaps more strongly, the need for working with materials of known composition and thermal history. It was therefore considered desirable to develop a glass preparation facility. A large part of the effort on the sulfide glasses is directed toward acquisition of the technology necessary for preparation of high purity samples and the development of quality control methods for this glass system.

The arsenic-sulfur system is selected for this study because,among the chalcogenide glasses,this system is perhaps best known due to frequent utilization in infrared applications. More specifically, from the available composition range, As_2S_3 was chosen because this is the only composition with an azeotropic maximum; this significantly reduces the problems of high purity preparation. Perhaps, most important, however, is the fact that various third element additions to As_2S_3 can significantly depress the softening point and thus provide a coating chemically similar to the As_2S_3 core.

A. MATERIALS PREPARATION

Purification by Distillation

Our method of purification is based on the phase diagram of arsenic and sulfur as presented in Hansen [22]. Figure 27 is a reproduction of that phase diagram. It shows an azeotropic maximum for As_2S_3. In fact, As_2S_3 is the only composition with a congruent boiling point between 32 and 100 atomic per cent sulfur. In the range 0 to 45.8 atomic per cent sulfur there is a nonvariant equilibrium at 535°C between solid arsenic, the saturated melt of 45.8 at. % S. and vapor of 32 at. % S.

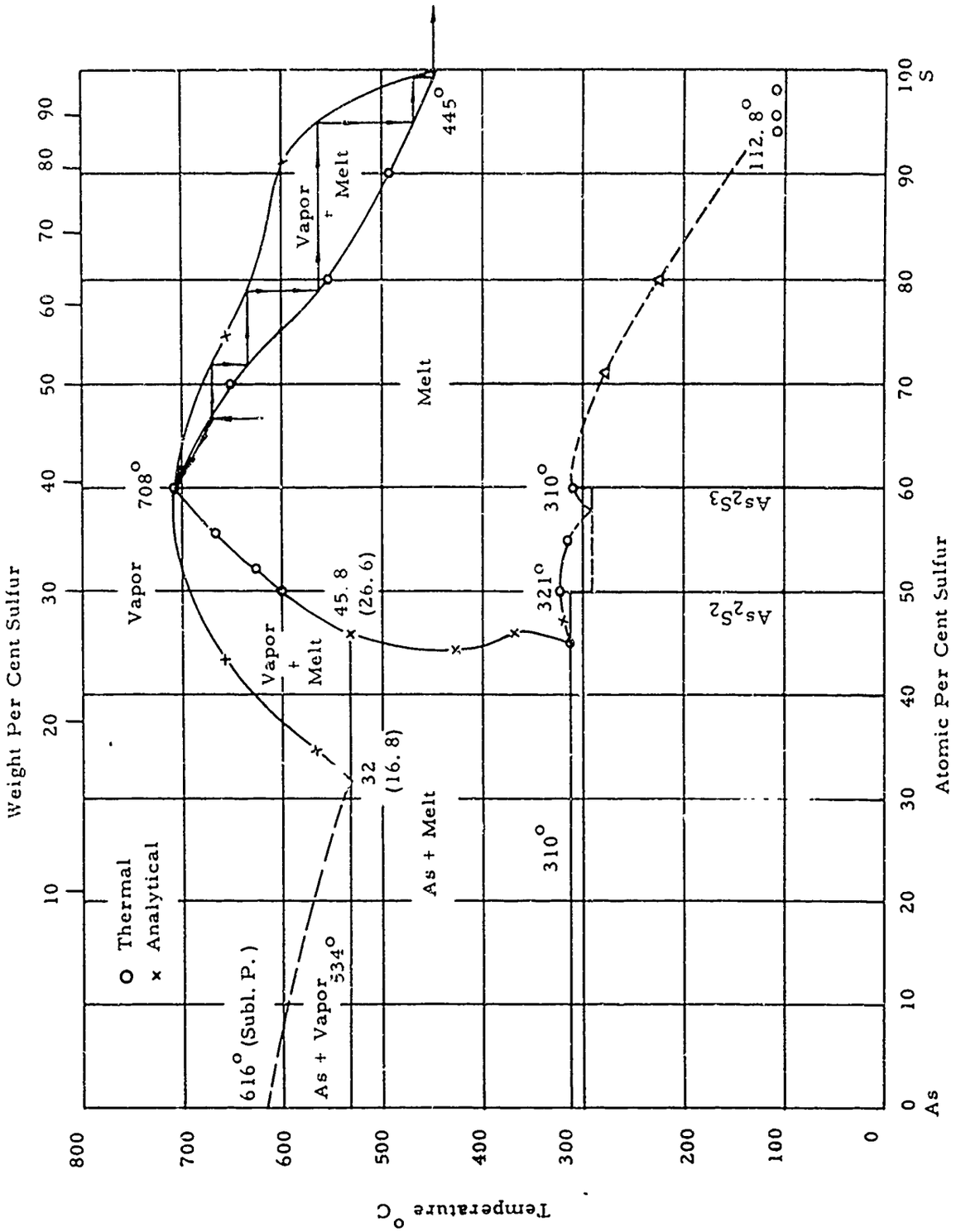

Figure 27. Phase diagram of arsenic-sulfur system.

If a composition of 67 at. % S is distilled, the first vapors arising from it will have a composition of 72 at. % S. This is the composition at the vapor end of the isothermal tie-line intersecting the lower (liquidus) curve at 67 at. % S. These vapors are condensed by the downward flowing liquid in the fractionation column which equilibrates with the vapor at each "plate" of the column. The condensed vapor then reboils producing a vapor of 79 at. % S which is found at the isothermal tie-line intersecting the liquidus at 72 at. % S. The new vapor is recondensed by the liquid in the column and again reboiled. This vapor has 95 at. % S and is, in turn, condensed further on up the column.

This reboiling and recondensation process is repeated at each "plate" in the column. After several such steps the composition of the vapor is pure sulfur. As sulfur is boiled away at the last "plate" at the top of the column, the liquid flowing down the column from the total reflux is condensed at the "drip tip" and collected. The remainder condenses at the walls and top of the head and flows down through the column.

The column then becomes an apparatus for bringing these streams into intimate contact, so that the vapor stream tends to vaporize the low-boiling constituent from the liquid, and the liquid stream tends to condense the high-boiling constituent from the vapor. Because the column is uniformly heated and the pot is operated hotter than the column, the top of the column is cooler than the bottom. The liquid stream becomes progressively hotter as it descends and the vapor stream becomes progressively cooler as it rises. This heat transfer is accomplished by actual contact of liquid and vapor.

As sulfur is continuously boiled away, the composition of the liquid draining from the column back into the pot follows the liquidus curve to the least volatile component, As_2S_3. The trend of the tie-lines shows that no matter what the original composition of the binary liquid between the azeotrope and sulfur, fractionation of the vapor will eventually give pure sulfur as the distillate and leave a residue of pure As_2S_3. This residue is distilled in a subsequent operation.

It is theoretically impossible to isolate the composition of intermediate volatility if sufficient "plates" are present and the column is operating with enough returning liquid for equilibration of each "plate". Any type of filling in the column that presents a larger surface of contact can be used instead of idealized "plates". Packed columns are about as effective as a sieve-plate or bubble-cap towers and have the advantages of low liquid hold up and small pressure drop. For narrow columns and vacuum distiliations they are superior to columns with actual plates.

Impurities are separated in the distillation according to their boiling points and vapor pressure curves with sulfur and As_2S_3. High boilers such as the metal sulfides and arsenides remain in the residue and are prevented from distilling over by the multiple plates of the column in the same way as As_2S_3 is prevented from distilling over with the sulfur. Antimony and aluminum, the principal impurities in the arsenic follow this rule. Low boilers distill over before or with the sulfur. These include arsenic oxide which sublimes at 1 atm. at 193°C. Intermediate boilers would come over between the As_2S_3 and sulfur fractions and would be removed with the sulfur which is collected with a small amount of As_2S_3 to assure its complete removal.

The operating temperatures of the "still" during the three phases of the distillation procedure are tabulated in Table IV.

TABLE IV

Distillation Apparatus Temperatures, °C

Thermocouple Position	Bake-out Phase	First Cut Phase	As_2S_3 Cut Phase
1	300	380	400
2	300	350	395
3	400	400	460
4	300	400	460
5	370	420	580
6	350	440	518
7	360	420	565
8	310	350	485
9	290	400	475
10	310	460	530
11	330	400	470

The consecutively numbered thermocouple positions are located in Figure 28. Initial bake-out to remove arsenic oxide, free sulfur, adsorbed gases, and other high vapor pressure contaminants is followed by distillation to remove sulfur and the lower boiling impurities. After 6 hours of this procedure the distillate is removed and the "still" restarted. Arsenic trisulfide is distilled at a faster rate by increasing the temperatures; the purity of the product is not compromised.

Figure 28 is a sketch of the distillate unit constructed entirely of Type 316 stainless steel. * Its two-foot column of 5/8"

---

* The initial version of the distillation unit was constructed of aluminum. However, contrary to literature reports, As_2S_3 attacks aluminum and the initial unit was replaced by one constructed entirely of stainless steel.

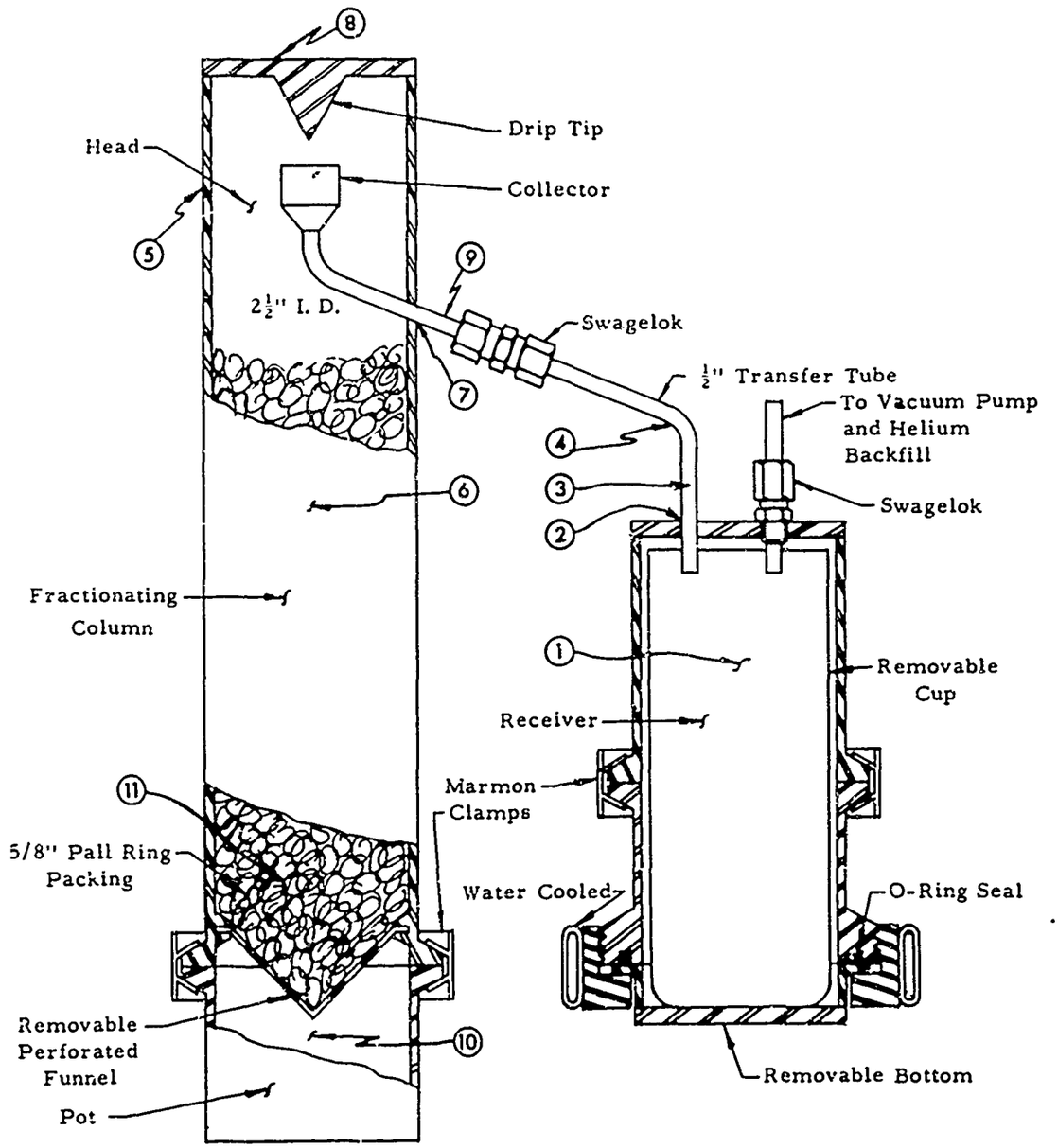

Figure 28. Fractional distillation unit, all 316 stainless steel.

all rings is equivalent to about 20 plates for an ideal fractionation column. The water-cooled bottom of the receiver is separable with a rubber O-ring seal. A steel cup inserted into the receiver provides a means of removing the entire distillate at any point in the process. When a cut is to be made, the transfer tube and receiver are air-cooled to rapidly freeze their contents, the receiver is back filled with high purity argon and the cup removed. Restarting is rapid and several cuts are readily obtained in one run.

Casting

Rods of pure arsenic sulfide glass are formed by melting the material obtained from the "still" in 6mm bore quartz tubes which have been pumped down to 10^{-5} mm Hg pressure and sealed. Following a program evolved from numerous experiments, the tubes are heated to 600°C and then cooled very slowly to 100°C, recycled, and quenched to room temperature. This program is found to produce bubble free rods of high uniformity.

B. EVALUATION OF MATERIAL

The interpretation of the mechanical properties of glasses is generally known to be limited by uncertainties of composition and impurity content. It was therefore considered desirable to explore a number of methods which could be applied individually at various stages of preparation and testing to determine specific properties relevant to the work in progress at that time. Three methods of analysis are listed below in order of increasing accuracy (and time required to perform the experiment).

(i) Density measurements

(ii) Infrared transmission

(iii) Chemical analyses

Of these, the first is most applicable for determining the composition of samples as they are produced and thereby detect any changes in preparation conditions as they occur. The second, infrared transmission, provides information on oxide impurity content and sample homogeneity. This method has evolved into a useful and comparatively fast quality control technique. An analytical technique which is expected to provide positive quality control of test specimens is being developed by the Sharp Schurtz Company. This technique should provide the first quantitative information on As_2S_3. The first two methods are discussed in more detail in the following.

Density Measurement

A relation between density and composition of arsenic sulfur glasses is reported by Tanaka and Minami [23]. Figure 29 is a reproduction of their curve based on gravimetric analysis of composition. This method reportedly yields reliable weight % determination of arsenic to about $\pm$ 0.3%. A hydrostatic technique, wherein the density is obtained by comparing the weight of a sample in air and water, was used to determine density. The ratio of the weight in air to the weight

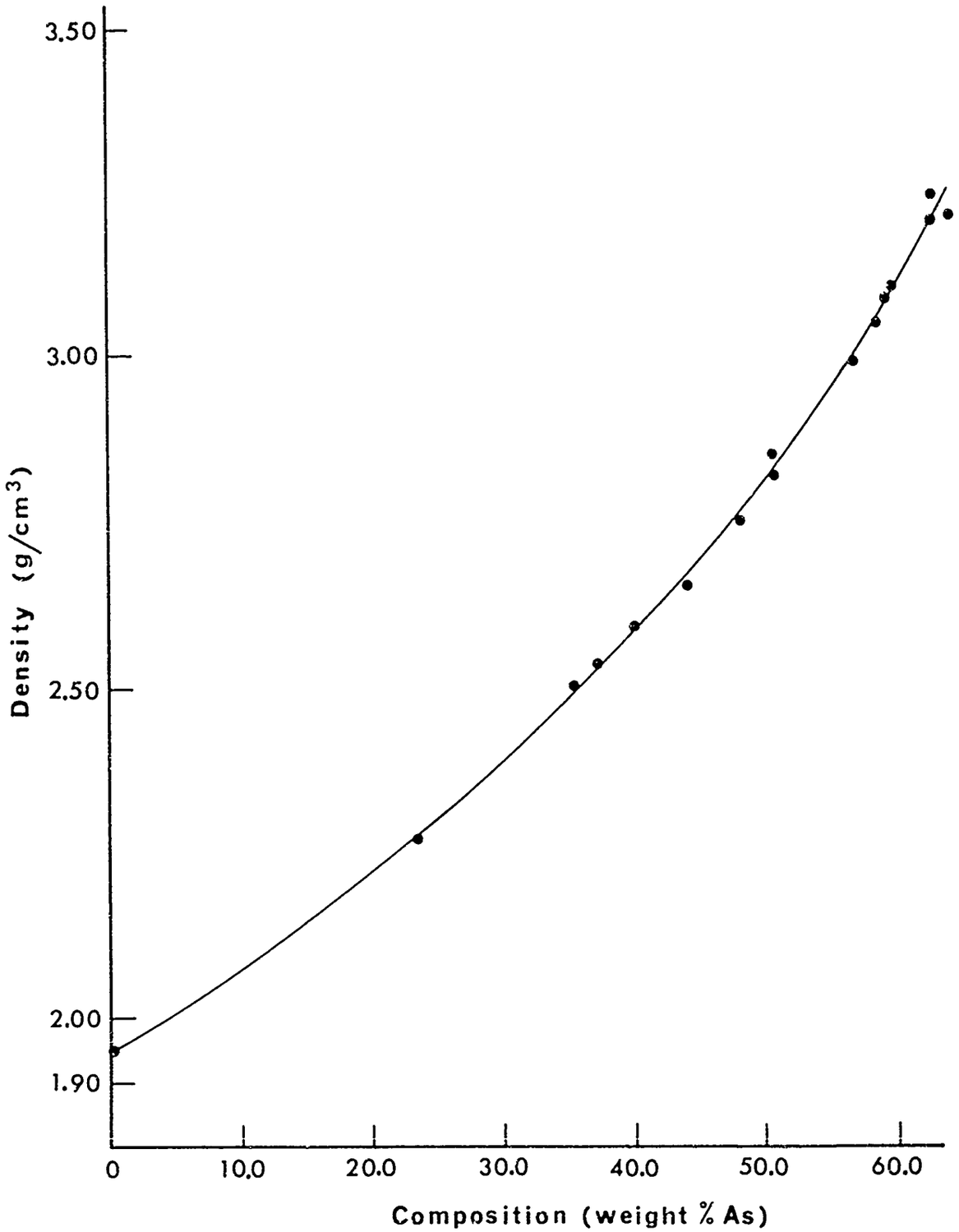

Figure 29. Composition dependence of density in arsenic-sulfur system. After (23).

in water (or any convenient liquid of known density) is given by

$$\frac{W_a}{W_w} = \frac{\rho - \rho_a}{\rho - \rho_w} \qquad (21)$$

where

ρ = true density of object weighed

ρ_a = density of air

ρ_w = density of water

For computation purposes this can be reduced to the more convenient form

$$\rho = \frac{W_a}{W_a - W_w} (\rho_w - \rho_a) + \rho_a \qquad (22)$$

Density values calculated from results of repeated weighings are within 0.1% of each other. Table V is a compilation of results obtained by this method using various specimens. Besides providing a direct method for compositional analysis, the density data can also be used to determine the quality of cast specimens. That is, by sectioning samples of known composition and determining the bubble content, a relation between density and homogeneity can be established.

Infrared Transmission

Considerable literature dealing with infrared transmission of As_2S_3 and correlations between various absorbtion bands and specific impurities is available. [24] Certain broad absorbtion bands (7 to 12 microns) can be correlated with sulfur content and impurity oxides.

The positions of impurity bands in sulfide glasses due to H-O, S-S,

TABLE V

Sample No.	Sample Origin	Preparation Conditions (All 1μ pressure except 1A)	Density g./c.c	Wt % As	Formula
1A	Residue	Simple distillation in vycor system	3.12	59.5	$AsS_{1.55}$
28	Distillate	First product of vacuum distillation not baked out	2.84	50	$AsS_{2.32}$
45A	Casting	Rod vacuum cast at 600°C in quartz tube	2.98	56	$AsS_{1.85}$
45B	Same casting	Front tip of above rod, lighter in color	2.86	51	$AsS_{2.25}$
29	Distillate	Product after preliminary vacuum bake out of system at 300°C	3.13	60	$AsS_{1.53}$
43	Casting	Rod formed by vacuum melting at 600°C in quartz tube	3.13	60	$AsS_{1.53}$
32A	Reaction product	Insufficiently reacted preparation	3.46	>65	
32B		Two samples taken	2.32	25	$AsS_{6.8}$
46A	Distillate	First product after preliminary 2 hour 300°C — dark glossy	3.11	59	$AsS_{1.60}$
		Vacuum bake out. Product not homogenous — light glossy	3.12	59.5	$AsS_{1.55}$
		crystalline	3.29	64	$AsS_{1.3}$
46B	Distillate	Second product at a higher vacuum distillation temperature	3.12	59.5	$AsS_{1.55}$
47A	Casting from distillate 29	Rod formed by vacuum casting at 610°C	3.19	61	$AsS_{1.45}$
47B		into 400° quartz tube;	3.14	60	$AsS_{1.50}$
47C		three sections measured	3.20	61	$AsS_{1.45}$
48A	Distillate	First product, prelim. bake-out 360°C distillation temperature (carry-over from previous run)	3.44	65	$AsS_{1.2}$
48B	Distillate	Second product, 460°C vacuum distillation two samples taken	3.09	59	$AsS_{1.60}$
			3.12	59.5	$AsS_{1.55}$
50A	Distillate	First product, 380°C vacuum distillation	3.17	61	$AsS_{1.45}$
50B	Distillate	Second product, 445°C vacuum distillation	3.20	61	$AsS_{1.45}$
50C	Distillate	Third product, 465°C vacuum distillation	3.20	61	$AsS_{1.45}$
50D	Residue	Remains in still	3.19	61	$AsS_{1.45}$
51D	Reaction product	Excess sulfur, 700°C reaction, 24 hours; homogenous	2.93	53.5	$AsS_{2.0}$

and As-O bonds are listed in Table VI.

TABLE VI

Position of "Impurity Bands" in Sulfide Glasses[24]

Source	H-O	S-S	As-O
Wavelength (Microns)	2.9		
	6.3		
		7.7	
			7.9
			8.7
			9.6
		10.15	
		10.75	
		11.9	
			12.8

Figure 30 shows the comparison of infrared transmittance of two different distillates and a commercial material. The generally higher curve, Run No. 31-28, resulted from a distillate which was baked out prior to distillation while the lower curve, Run No. 31-26, was cast directly. The slower distillation procedure, Run No. 31-28, clearly produces a material of greater purity; note, in particular, the absence of the 8.7 micron As-O absorbtion band.

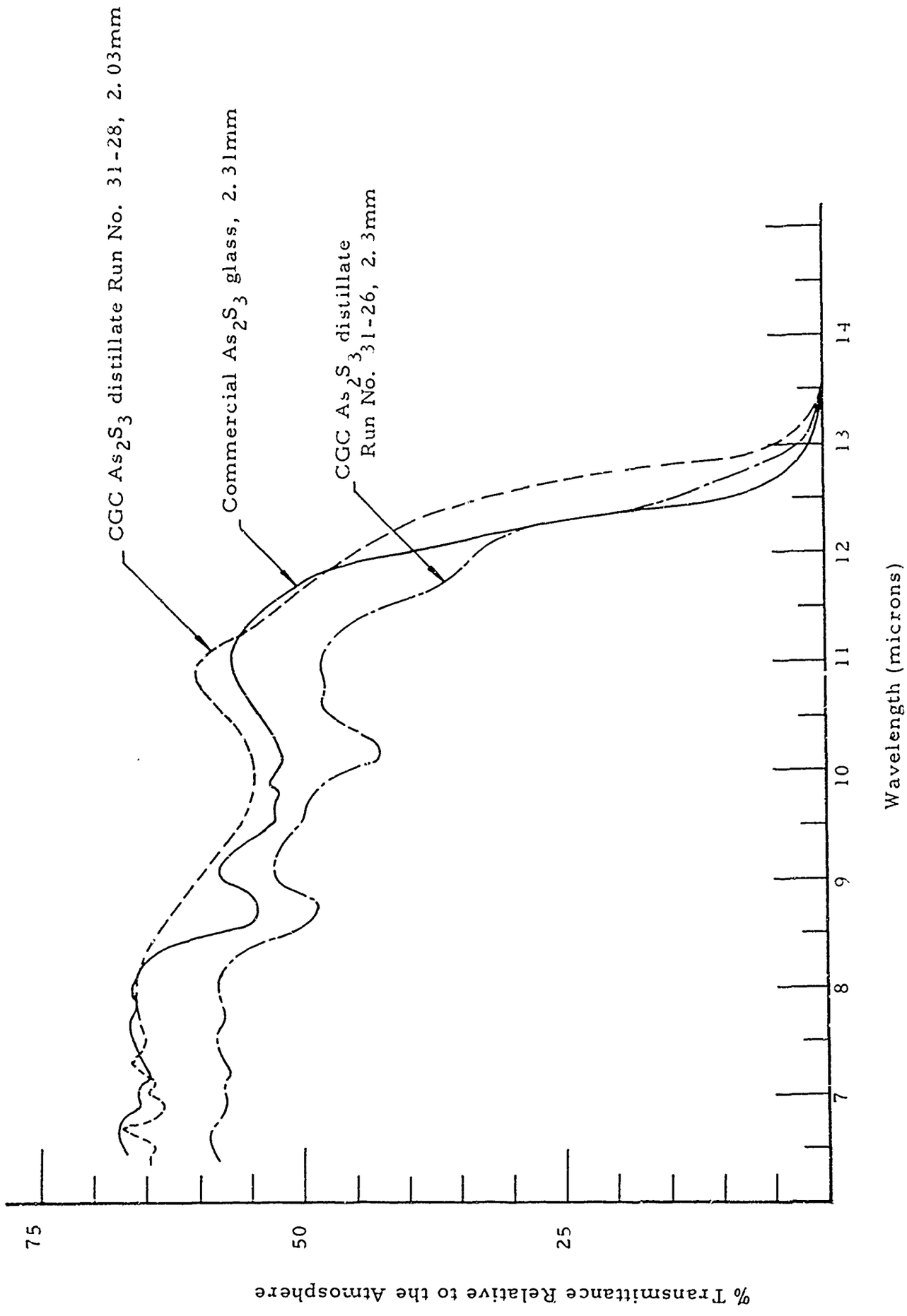

Figure 30. Relative transmittance of two distillates compared to commercial arsenic trisulfide.

C. LOW MELTING POINT GLASS COATINGS

A number of arsenic-sulfur-third element ternaries have been evaluated for potential use on As_2S_3 cast rods. The following desired systems properties serve as guidelines in the selection and evaluation process:

(i) The As_2S_3 core and As-S-X coating remain compositionally stable over the temperature interval required for composite preparation and testing.

(ii) Low tendency toward crystallization of core and coating.

(iii) Viscosity of the outer coating composition remain below 10^{14} poises near 25°C ($10^{14.5}$ defined as the softening temperature).

(iv) The chemical interaction of the core and coating produce a continuous interface at the treatment temperature.

Of those considered, the arsenic-sulfur-iodine glass system appears to be the most promising. Unlike the sulfide and selenide glasses, As-S-I resists oxidation in air up to 300°C. High sulfur compositions have a tendency toward immiscibility and low sulfur preparations exhibit crystalline phase formation. The most promising composition, (1.167 As) (0.587S) (0.246I) mole fraction, remains fluid over the temperature interval from below 0° to 100°C. Some degree of crystallization is observed at temperatures between 30°and 50°C. The process is visible after one hour and progresses to a tacky state after four hours. Above 60°C and below 25°C no change in appearance is noticed even after several days exposure. While further studies of this system and other systems are continuing, it now appears that sufficient control of the coating glass is possible to initiate the strength studies.

LITERATURE CITED

1. Griffith, A. A., Phil. Trans. Roy. Soc., London, 221A, 163 (1920).

2. Otto, W. H. and Preston, F. W., J. Soc. Glass Technol., 34, 63 (1950).

3. Tool, A. Q., as cited in, Powell, H. E. and Preston, F. W., J. Am. Ceram. Soc., 28, 145 (1945).

4. Hillig, W. B., Modern Aspects of the Vitreous State, edited by J. D. Mackenzie, Butterworths, Washington, 1962.

5. Ernsberger, F. M. and Braithwaite, D. Ct., J. Am. Ceram. Soc., 39, 471 (1960).

6. Zijlstra, A. L., Symposium sur la résistance mécanique du verre et les moyens de l'ameliorer, Union Scientifique Continentale du verre, Belgique, 1961.

7. Bartenev, T. A., et. al., Zh. Fizi Khim., 29, 508 (1955).

8. Proctor, B., Phys. Chem. Glasses, 3, 7 (1962).

9. Timoshenko, S., Strength of Materials, Part II, D. Van Nostrand Co., Inc., New York, 1956.

10. Stevels, J. M., Handbuch Der Physik, Vol. 13, Springer-Verlag, Berlin, 1962.

11. Landau, L. D. and Lifshitz, E. M., Theory of Elasticity, Pergamon Press, London, 1959.

12. Holland, L., The Properties of Glass Surfaces, Chapt IV, John Wiley and Sons, Inc., New York, 1964.

13. Oldfield, L. F. and Wright, R. D., Advances In Glass Technology, V, International Congress On Glass, Plenum Press, New York, 1962.

14. Tool, A. Q. and Eichlin, D. G., U. S. Standards Bureau Journal of Research, 6 (1931).

15. Nemilov, S. V., Soviet Physics Solid State, 6, 1075 (1964). English translation.

16. Lillie, H. R., J. Am. Ceram. Soc., 16, 619 (1933).

17. Dale, A. E. and Stanworth, J. E., J. Soc. Glass Technol., 28, 414 (1945).

18. Stanworth, J. E., Physical Properties of Glass, Oxford, London, 1953.

19. More, G. W., The Properties of Glass, Reinhold Publishing Corp., New York, 1954.

20. Robinson, D. M., Physics, 2, 52 (1932).

21. Sutton, P. M., J. Am Ceram. Soc., 47, 188, 219 (1964).

22. Hansen, M., Constitution of Binary Alloys, McGraw-Hill, New York, 1958.

23. Tanaka, M., Minami, T., Jap. J. Appl. Phys., 4, 939 (1965).

24. Savage, J. A., and Nielsen, S., Infrared Physics, 5, 195 (1965).

Security Classification

DOCUMENT CONTROL DATA - R&D

(Security classification of title, body of abstract and indexing annotation must be entered when the overall report is classified)

1 ORIGINATING ACTIVITY *(Corporate author)*
Cadillac Gage Co., Research Division
20316 Hoover Road
Detroit, Michigan 48205

2a REPORT SECURITY CLASSIFICATION
Unclassified

2b GROUP

3 REPORT TITLE
INVESTIGATION OF ULTRA HIGH STRENGTH BULK GLASS

4 DESCRIPTIVE NOTES *(Type of report and inclusive dates)*
Final Report March 1965 through March 1966

5 AUTHOR(S) *(Last name, first name, initial)*
Teeg, Robert, O. Zucker, Gordon, L. Hallman, Robert, W.

6 REPORT DATE	7a TOTAL NO OF PAGES	7b NO OF REFS
15 April 1966	70 p.	24

8a CONTRACT OR GRANT NO	9a ORIGINATOR'S REPORT NUMBER(S)
NOw 65-0388-f	900-008
b. PROJECT NO	
c	9b OTHER REPORT NO(S) *(Any other numbers that may be assigned this report)*
d.	

10 AVAILABILITY/LIMITATION NOTICES
DISTRIBUTATION OF THIS DOCUMENT IS UNLIMITED

11 SUPPLEMENTARY NOTES	12 SPONSORING MILITARY ACTIVITY
	Bureau of Naval Weapons (Department of the Navy)

13 ABSTRACT

A technique is described by which the intrinsic strength of bulk glass can be measured. The technique is applied to examine the factors which influence the engineering strength of glass. Results of tensile strength measurements on bulk borosilicate glasses, obtained by bending tests, approach theoretical values. Measurement of the temperature dependence of strength in the range 350° to 600°C reveals an interesting strength-temperature transformation. Electrical measurements are also performed in this temperature range in an effort to interrelate electrical and mechanical behavior. Sulfide glass preparation and evaluation techniques are described to provide test specimen composites capable of exhibiting intrinsic strength near room temperature.

DD FORM 1 JAN 64 1473

Security Classification

14. KEY WORDS	LINK A		LINK B		LINK C	
	ROLE	WT	ROLE	WT	ROLE	
GLASS MECHANICAL PROPERTIES OF GLASS HIGH STRENGTH GLASS INTRINSIC STRENGTH OF GLASS BOROSILICATE AND SULFIDE GLASSES PROPERTIES OF PROTECTED GLASS HIGH STRENGTH COMPOSITES ELECTRICAL PROPERTIES OF GLASS						

INSTRUCTIONS

1. ORIGINATING ACTIVITY Enter the name and address of the contractor, subcontractor, grantee, Department of Defense activity or other organization *(corporate author)* issuing the report.

2*a*. REPORT SECURITY CLASSIFICATION: Enter the overall security classification of the report. Indicate whether "Restricted Data" is included. Marking is to be in accordance with appropriate security regulations.

2*b*. GROUP: Automatic downgrading is specified in DoD Directive 5200.10 and Armed Forces Industrial Manual. Enter the group number. Also, when applicable, show that optional markings have been used for Group 3 and Group 4 as authorized.

3. REPORT TITLE: Enter the complete report title in all capital letters. Titles in all cases should be unclassified. If a meaningful title cannot be selected without classification, show title classification in all capitals in parenthesis immediately following the title.

4. DESCRIPTIVE NOTES. If appropriate, enter the type of report, e.g., interim, progress, summary, annual, or final. Give the inclusive dates when a specific reporting period is covered.

5. AUTHOR(S): Enter the name(s) of author(s) as shown on or in the report. Enter last name, first name, middle initial. If military, show rank and branch of service. The name of the principal author is an absolute minimum requirement.

6. REPORT DATE. Enter the date of the report as day, month, year, or month, year. If more than one date appears on the report, use date of publication.

7*a*. TOTAL NUMBER OF PAGES: The total page count should follow normal pagination procedures, i.e., enter the number of pages containing information.

7*b*. NUMBER OF REFERENCES. Enter the total number of references cited in the report.

8*a*. CONTRACT OR GRANT NUMBER. If appropriate, enter the applicable number of the contract or grant under which the report was written.

8*b*, 8*c*, & 8*d*. PROJECT NUMBER: Enter the appropriate military department identification, such as project number, subproject number, system numbers, task number, etc.

9*a*. ORIGINATOR'S REPORT NUMBER(S): Enter the official report number by which the document will be identified and controlled by the originating activity. This number must be unique to this report.

9*b*. OTHER REPORT NUMBER(S): If the report has been assigned any other report numbers *(either by the originator or by the sponsor)*, also enter this number(s).

10. AVAILABILITY LIMITATION NOTICES. Enter any limitations on further dissemination of the report, other than those imposed by security classification, using standard statements such as:

(1) "Qualified requesters may obtain copies of this report from DDC."

(2) "Foreign announcement and dissemination of this report by DDC is not authorized."

(3) "U. S. Government agencies may obtain copies of this report directly from DDC. Other qualified DDC users shall request through _____."

(4) "U. S. military agencies may obtain copies of this report directly from DDC. Other qualified users shall request through _____."

(5) "All distribution of this report is controlled. Qualified DDC users shall request through _____."

If the report has been furnished to the Office of Technical Services, Department of Commerce, for sale to the public, indicate this fact and enter the price, if known.

11. SUPPLEMENTARY NOTES. Use for additional explanatory notes.

12. SPONSORING MILITARY ACTIVITY: Enter the name of the departmental project office or laboratory sponsoring *(paying for)* the research and development. Include address.

13 ABSTRACT Enter an abstract giving a brief and factual summary of the document indicative of the report, even though it may also appear elsewhere in the body of the technical report. If additional space is required, a continuation sheet shall be attached.

It is highly desirable that the abstract of classified reports be unclassified. Each paragraph of the abstract shall end with an indication of the military security classification of the information in the paragraph, represented as *(TS)*, *(S)*, *(C)*, or *(U)*.

There is no limitation on the length of the abstract. However, the suggested length is from 150 to 225 words.

14 KEY WORDS Key words are technically meaningful terms or short phrases that characterize a report and may be used as index entries for cataloging the report. Key words must be selected so that no security classification is required. Identifiers, such as equipment model designation, trade name, military project code name, geographic location, may be used as key words but will be followed by an indication of technical context. The assignment of links, rules, and weights is optional.